

$\beta_2$ -adrenoceptor-induced modulation of  
transglutaminase 2 transamidase activity in cardiomyoblasts

Falguni S. VYAS<sup>a</sup>, Carl P. NELSON<sup>a</sup>, Fiona FREEMAN<sup>a</sup>, David J. BOOCOCK<sup>b</sup>, Alan J  
HARGREAVES<sup>a</sup>, John M. DICKENSON<sup>a\*</sup>

<sup>a</sup>School of Science and Technology  
Nottingham Trent University  
Clifton Lane  
Nottingham  
NG11 8NS

<sup>b</sup> John van Geest Cancer Research Centre  
Nottingham Trent University  
Clifton Lane  
Nottingham  
NG11 8NS

\*To whom correspondence should be addressed

Tel: +44-1158486683

E-mail: [john.dickenson@ntu.ac.uk](mailto:john.dickenson@ntu.ac.uk)

Running title:  $\beta_2$ -adrenoceptor-induced TG2 activation

## **Abstract**

Tissue transglutaminase 2 (TG2) is modulated by protein kinase A (PKA) mediated phosphorylation: however, the precise mechanism(s) of its modulation by G-protein coupled receptors coupled to PKA activation are not fully understood. In the current study we investigated the potential regulation of TG2 activity by the  $\beta_2$ -adrenoceptor in rat H9c2 cardiomyoblasts. Transglutaminase transamidation activity was assessed using amine-incorporating and protein cross-linking assays. TG2 phosphorylation was determined via immunoprecipitation and Western blotting. The long acting  $\beta_2$ -adrenoceptor agonist formoterol induced time- and concentration-dependent increases in TG2 transamidation. Increases in TG2 activity were reduced by the TG2 inhibitors Z-DON (Benzyloxycarbonyl-(6-Diazo-5-oxonorleuciny)-L-valinyl-L-prolinyl-L-leucinmethylester) and R283 (1,3-dimethyl-2[2-oxo-propyl]thio)imidazole chloride). Responses to formoterol were blocked by pharmacological inhibition of PKA, extracellular signal-regulated kinase 1 and 2 (ERK1/2), or phosphatidylinositol 3-kinase (PI-3K) signalling. Furthermore, the removal of extracellular  $\text{Ca}^{2+}$  also attenuated formoterol-induced TG2 activation. Fluorescence microscopy demonstrated TG2-induced biotin-X-cadaverine incorporation into proteins. Formoterol increased the levels of TG2-associated phosphoserine and phosphothreonine, which were blocked by inhibition of PKA, ERK1/2 or PI-3K signalling. Subsequent proteomic analysis identified known (e.g. lactate dehydrogenase A chain) and novel (e.g. Protein S100-A6) protein substrates for TG2. Taken together, the data obtained suggest that  $\beta_2$ -adrenoceptor-induced modulation of TG2 represents a novel paradigm in  $\beta_2$ -adrenoceptor cell signalling, expanding the repertoire of cellular functions responsive to catecholamine stimulation.

**Key words:**  $\beta_2$ -adrenoceptor; phosphorylation; protein kinase A; ERK1/2; H9c2 cardiomyocytes; transglutaminase 2.

## 1. Introduction

Transglutaminases (EC 2.3.2.13; TGs) are a family of structurally and functionally similar  $\text{Ca}^{2+}$  dependent enzymes that catalyse post-translational modifications of proteins. TGs introduce a stable covalent bond between free amine groups (e.g. protein- or peptide-bound lysine) and  $\gamma$ -carboxamide groups of peptide-bound glutamine residues (Eckert et al., 2014). Nine members of the TG family have been characterised (Factor XIIIa, TGs 1-7 and erythrocyte band 4.2), of which erythrocyte band 4.2 is inactive in mammals (Iismaa et al., 2009; Agnihotri and Mehta, 2017). TG2 is the only member of the family that is ubiquitously expressed and displays a variety of activities. Along with post-translational protein modifications (transamidation, deamidation, protein disulphide isomerase), TG2 also acts as a G-protein ( $G_h$ ) and has an intrinsic kinase activity (Gundemir et al., 2012).

When acting as a G-protein, TG2 couples to members of the G-protein coupled receptor (GPCR) family including the  $\alpha_{1\beta}$ -adrenergic receptor, thromboxane A2 receptor and oxytocin receptor (Gundemir et al., 2012). The capacity of TG2 to perform multifunctional roles in cells and tissues makes it an important regulator of many cellular functions, including migration, cell adhesion, cell differentiation, cell survival, apoptosis, and organization of the extracellular matrix (Nurminskaya and Belkin, 2012). Dysregulation of TG2 is implicated in numerous pathologies, e.g. celiac disease, neurodegenerative disorders, cancer and fibrosis; hence, it represents a potential therapeutic target (Caccamo et al., 2010). TG2 activity is modulated by protein kinases; e.g. phosphorylation of TG2 at Ser<sup>216</sup> by protein kinase A (PKA) inhibits its transamidase activity and enhances its kinase activity (Mishra et al., 2007; Wang et al., 2012). However at present, the precise mechanism(s) of its modulation by GPCRs coupled to PKA activation are not fully understood.

The  $\beta_2$ -adrenoceptor is a member of the GPCR superfamily, which can interact with both  $G_s$  and  $G_i$ -proteins (Rockman et al., 2002). When interacting with  $G_s$ , the  $\beta_2$ -adrenoceptor activates PKA-dependent signalling pathway (Benovic, 2002). Interaction with  $G_i$  results in the release of  $\beta\gamma$  subunits and triggers the activation of additional signaling cascades that

include extracellular signal-regulated kinase 1 and 2 (ERK1/2) and protein kinase B (PKB; Daaka et al., 1997; Okamoto et al., 1991; Steinberg, 1999; Yano et al., 2007). Our recent studies have demonstrated that TG2 activity increases in cardiomyocyte-like H9c2 cells following stimulations with phorbol-12-myristate-13-acetate (PMA) and forskolin, activators of protein kinase C (PKC) and PKA, respectively (Almami et al., 2014). Overall, these observations indicate that TG2 activity could be modulated by the  $\beta_2$ -adrenoceptor. In this respect, it is interesting to note that  $\beta_2$ -adrenoceptor activation triggers TG2 expression in macrophages in response to the stress-related catecholamines adrenaline and noradrenaline (Yanagawa et al., 2014). In the present study, we have demonstrated for the first time that activation of the  $\beta_2$ -adrenoceptor with the long-acting  $\beta_2$ -adrenoceptor agonist formoterol increases TG2 transamidation activity in H9c2 cells via a pathway dependent upon PKA, ERK1/2, phosphatidylinositol 3-kinase (PI-3K) and extracellular  $\text{Ca}^{2+}$ . Hence  $\beta_2$ -adrenoceptor-induced modulation of TG2 represents a novel paradigm in  $\beta_2$ -adrenoceptor cell signalling, expanding the repertoire of cellular functions responsive to catecholamine stimulation.

## 2. Materials and methods

### 2.1. Materials

AS 605240 (5-(6-Quinoxalinylmethylene)-2,4-thiazolidine-2,4-dione), BAPTA/AM (1,2-Bis(2-aminophenoxy)ethane-*N,N,N',N'*-tetraacetic acid tetrakis acetoxymethyl ester), CGP 20712 (1-[2-((3-Carbamoyl-4-hydroxy)phenoxy)ethylamino]-3-[4-(1-methyl-4-trifluoromethyl-2-imidazolyl)phenoxy]-2-propanol dihydrochloride), CL 316243 (5-[(2*R*)-2-[[2*R*)-2-(3-Chlorophenyl)-2-hydroxyethyl]amino]propyl]-1,3-benzodioxole-2,2-dicarboxylic acid disodium salt), dobutamine, formoterol, ICI 118,551 ( $\pm$ )-*erythro*-(*S*\*,*S*\*)-1-[2,3-(Dihydro-7-methyl-1*H*-inden-4-yl)oxy]-3-[(1-methylethyl)amino]-2-butanol hydrochloride), KT 5720 (9*R*,10*S*,12*S*)-2,3,9,10,11,12-Hexahydro-10-hydroxy-9-methyl-1-oxo-9,12-epoxy-1*H*-diindolo[1,2,3-*fg*:3',2',1'-*kl*]pyrrolo[3,4-*i*][1,6]benzodiazocine-10-carboxylic acid, hexyl ester), LY 294002 (2-(4-morpholinyl)-8-phenyl-4*H*-1-benzopyran-4-one), PD 98059 (2'-amino-3'-methoxyflavone), propranolol and wortmannin were obtained from Tocris Bioscience (Bristol, UK). Casein, 3-isobutyl-1-methylxanthine (IBMX), *N,N'*-dimethylcasein, pertussis toxin, protease inhibitor cocktail, phosphatase inhibitor cocktail 2, horseradish peroxidase conjugated ExtrAvidin® (ExtrAvidin-HRP), Fluorescein isothiocyanate-conjugated ExtrAvidin® (ExtrAvidin-FITC and Triton™ X-100 was obtained from Sigma-Aldrich Company Ltd. (Gillingham, UK). The TG2 inhibitors Z-DON (Z-DON-Val-Pro-Leu-OMe; Benzyloxycarbonyl-(6-Diazo-5-oxonorleucinyl)-L-valinyl-L-prolinyl-L-leucinmethylester) and R283 (1,3-dimethyl-2[2-oxo-propyl]thio)imidazole chloride) along with purified standard guinea-pig liver TG2 were obtained from Zedira GmbH (Darmstadt, Germany). Biotin-TVQQEL was purchased from Pepceuticals (Enderby, UK). Biotin cadaverine (N-(5-aminopentyl)biotinamide) and biotin-X-cadaverine (5-[(N-(biotinoyl)amino)hexanoyl]amino)pentylamine) were purchased from Invitrogen UK (Loughborough, UK). DAPI (2-[4-(Aminoiminomethyl)phenyl]-1*H*-Indole-6-carboximidamide hydrochloride) was from Vector Laboratories Inc (Peterborough, UK). Coomassie blue

(InstantBlue™ stain) was purchased from Expedeon (Swavesey, UK). Fluo-8 AM was purchased from Stratech Scientific Ltd (Newmarket, UK). Rp-cAMPs (adenosine 3',5'-cyclic monophosphorothioate, 8-chloro, Rp-isomer) was from Calbiochem (San Diego, CA, USA). Dulbecco's modified Eagle's medium (DMEM), foetal bovine serum, trypsin (10X), L-glutamine (200 mM), penicillin (10,000 U/ml)/streptomycin (10,000 µg/ml) were purchased from Lonza (Castleford, UK). All other reagents were purchased from Sigma-Aldrich Co Ltd (Gillingham, UK) and were of analytical grade. Antibodies were obtained from the following suppliers: monoclonal phospho-specific ERK1/2 (Thr<sup>202</sup>/Tyr<sup>204</sup>) from Sigma-Aldrich; polyclonal phospho-specific PKB (Ser<sup>473</sup>), polyclonal total unphosphorylated PKB, monoclonal total unphosphorylated ERK1/2, polyclonal total unphosphorylated c-Jun N-terminal kinase (JNK), polyclonal total unphosphorylated p38 mitogen-activated protein kinase (p38 MAPK), monoclonal phospho-specific p38 MAPK, monoclonal phospho-specific JNK, and polyclonal anti-cleaved caspase 3 from New England Biolabs (UK) Ltd (Hitchin, UK); monoclonal anti-transglutaminase 2 (CUB 7402) from Thermo Scientific (Loughborough, UK); polyclonal antibodies recognising phosphoserine and phosphothreonine from Abcam (Cambridge, UK).

## **2.2. Cell culture**

Rat embryonic cardiomyoblast-derived H9c2 cells were obtained from the European Collection of Animal Cell Cultures (Porton Down, Salisbury, UK). These cells, derived from embryonic rat heart tissue (Kimes and Brandt, 1976), are increasingly used as an *in vitro* model for studies exploring cardioprotection, since they display similar morphological, electrophysiological and biochemical properties to primary cardiac myocytes (Hescheler et al., 1991). Cells were cultured in 75 cm<sup>2</sup> flasks in DMEM supplemented with 2 mM L-glutamine, 10% (v/v) foetal bovine serum and penicillin (100 U/ml)/streptomycin (100 µg/ml). Cells were maintained at 37°C in a humidified 5% CO<sub>2</sub> atmosphere until confluency and sub-cultured (1:10 split ratio) using trypsin (0.05% w/v)/EDTA (0.02% w/v).

### **2.3. RT-PCR analysis of $\beta_1$ , $\beta_2$ and $\beta_3$ -adrenoceptor mRNA expression**

Total RNA was isolated from mitotic H9c2 cells, rat heart and rat lung using a GenElute™ mammalian total RNA isolation miniprep kit (Sigma-Aldrich Company Ltd, Gillingham, UK) according to the manufacturer's instructions. First strand complementary DNA (cDNA) was synthesized utilising random primers and M-MLV reverse transcriptase (Promega, Southampton, UK). PCR was performed using the following gene-specific primer sequences:  $\beta_1$ -adrenoceptor (599 bp cDNA product) forward 5'-TACTCCTGGCGCTCATCGT-3' and reverse 5'-CTCGCAGCTGTTCGATCTTC-3';  $\beta_2$ -adrenoceptor (323 bp cDNA product) forward 5'-AGCCACACGGGAATGACAG-3' and reverse 5'-CCAGAACTCGCACCAGAA-3';  $\beta_3$ -adrenoceptor (724 bp cDNA product) forward 5'-AGTCCTGGTGTGGATCGTG-3' and reverse 5'-ACGCTCACCTTCATAGCCAT-3'; GAPDH (392 bp cDNA product) forward 5'-CAAGTTCAACGGCACAGTCA-3' and reverse 5'-GAGTGGCAGTGATGGCATG-3'. PCR conditions for the  $\beta_1$ ,  $\beta_2$  and  $\beta_3$ -adrenoceptor and GAPDH were 40 cycles of 94°C for 1 min, 59°C for 1.5 min, and 72°C for 1 min. RT-PCR products were analysed by using 1.5% (w/v) agarose gel electrophoresis and visualised by ethidium bromide staining.

### **2.4. cAMP accumulation assay**

H9c2 cells (5000 cells/well) were seeded on a white 96 well microtitre plate, with clear-bottomed wells (Fisher Scientific, Loughborough, UK) and cultured for 24 h in fully supplemented DMEM. The medium was removed and the monolayer treated with a range of concentrations of formoterol for 20 min in serum-free DMEM (40  $\mu$ l/well) in the presence of 20 mM  $MgCl_2$  and 500  $\mu$ M IBMX. Following stimulation, cAMP levels within cells were determined using the cAMP-Glo™ Max Assay kit (Promega UK, Southampton, UK). Briefly, 10  $\mu$ l of cAMP detection solution were added to all wells and incubated for 20 min at room temperature. After incubation, Kinase-Glo® reagent (50  $\mu$ l/well) was added and incubated for 10 min at room temperature, following which luminescence levels across the plate were

read using a plate-reading FLUOstar Optima luminometer (BMG Labtech Ltd, Aylesbury, UK). Forskolin (10  $\mu$ M) was used as a positive control and the luminescence values were converted to cAMP levels using a cAMP standard curve (0-100 nM), according to the manufacturer's instructions.

## **2.5. Transglutaminase activity assays**

Time course profiles and concentration-response curves were obtained for formoterol. Where appropriate, cells were also pre-incubated for 30 min in a medium with or without the protein/lipid kinase inhibitors *Rp*-cAMPs (PKA, 50  $\mu$ M; de Wit et al., 1984), KT 5720 (PKA, 5  $\mu$ M; Kase et al., 1987), PD 98059 (MEK1/2, 50  $\mu$ M; Dudley et al., 1995), LY 294002 (PI-3K, 30  $\mu$ M; Vlahos et al., 1994), wortmannin (PI-3K; 100 nM; Arcaro and Wymann, 1993) and AS 605240 (PI-3K $\gamma$ ; 1  $\mu$ M; Camps et al., 2005) prior to treatment with 1  $\mu$ M formoterol. Following stimulation, cells were rinsed twice with 2.0 ml of chilled PBS, lysed with 500  $\mu$ l of ice-cold lysis buffer (50 mM Tris-HCl pH 8.0, 0.5% (w/v) sodium deoxycholate, 0.1% (v/v) protease inhibitor cocktail, and 1% (v/v) phosphatase inhibitor cocktail 2 and 3). Cell lysates were clarified by centrifugation at 4°C for 10 min at 14,000 x g prior to being assayed for TG activity, as described below. Protein was determined using the bicinchoninic acid (BCA) protein assay (Smith et al., 1985), using a commercially available kit (Sigma-Aldrich Co. Ltd), with bovine serum albumin (BSA) as the standard.

Biotin-labelled cadaverine incorporation assays were performed according to Slaughter et al. (1992) with the modifications reported by Lilley et al. (1998). Briefly, 96-well microtitre plates were coated overnight at 4° C with 250  $\mu$ l of N',N'-dimethylcasein (10 mg/ml in 100 mM Tris-HCl, pH 8.0). The plate was washed twice with distilled water, blocked with 250  $\mu$ l of 3% (w/v) BSA in 100 mM Tris-HCl, pH 8.0 and incubated for 1 h at room temperature. The plate was washed twice before the application of 150  $\mu$ l of either 6.67 mM calcium chloride or 13.3 mM EDTA (used to check background TG2 activity) assay buffer containing 225  $\mu$ M biotin-cadaverine (a widely used substrate to monitor TG amine

incorporating activity) and 2 mM 2-mercaptoethanol. The reaction was started by the addition of 50 µl of samples, positive control (50 ng/well of guinea-pig liver TG2) and/or negative control (100 mM Tris-HCl, pH 8.0). After incubation for 1 h at 37°C, plates were washed as before. Then, 200 µl of 100 mM Tris-HCl pH 8.0 containing 1% (w/v) BSA and ExtrAvidin®-HRP (1:5000 dilution) were added to each well and the plate incubated at 37°C for 45 min; it was then washed as before. The plate was developed with 200 µl of freshly prepared developing buffer (7.5 µg/ml 3, 3', 5, 5'-tetramethylbenzidine and 0.0005% (v/v) H<sub>2</sub>O<sub>2</sub> in 100 mM sodium acetate, pH 6.0) and incubated at room temperature for 15 min. The reaction was terminated by adding 50 µl of 5.0 M sulphuric acid and the absorbance read at 450 nm. One unit of TG2 was defined as a change in absorbance of one unit/h. Each experiment was performed in triplicate.

Biotin-labelled peptide cross-linking assay was performed according to the method of Trigwell et al. (2004) with minor modifications. Microtitre plates (96-well) were coated and incubated overnight at 4°C with casein at 1 mg/ml in 100 mM Tris-HCl pH 8.0 (250 µl per well). The wells were washed twice with distilled water, before incubation at room temperature for 1 h with 250 µl of blocking solution (100 mM Tris-HCl pH 8.0 containing 3% (w/v) BSA). The plate was washed twice before the application of 150 µl of either 6.67 mM calcium chloride or 13.3 mM EDTA assay buffer containing 5 µM biotin-TVQQEL and 2 mM 2-mercaptoethanol. Starting of reactions, positive and negative controls, reaction development and termination were as described above for biotin-cadaverine assay. One unit of TG2 was defined as a change in absorbance of one unit/h. Each experiment was performed in triplicate.

## **2.6. Western blot analysis**

H9c2 cells were grown in 25 cm<sup>2</sup> flasks and when 80-90% confluent placed in serum free DMEM medium for 16 h. Serum-starved cells were then washed once with PBS (pH 7.4) and where appropriate incubated for 30 min in medium with or without the protein/lipid kinase

inhibitors as described above, prior to treatment with 1  $\mu\text{M}$  formoterol. Following treatment cells were washed twice with PBS and lysed (300  $\mu\text{l}$ ) with boiling 0.5% (w/v) SDS in Tris. Protein samples (15-20  $\mu\text{g}$ ) were separated by SDS-PAGE in 10% (w/v) polyacrylamide gels using a Bio-Rad Mini Protean III system. Proteins were transferred to nitrocellulose membranes in a Bio-Rad Trans-Blot system, using electro-transfer buffer comprising 25 mM Tris, 192 mM glycine pH 8.3 and 20% (v/v) MeOH. Following transfer, the membranes were blocked and probed with antibodies as described by Almami et al., (2014). The primary antibodies (1:500 dilutions unless otherwise indicated) used were phospho-specific ERK1/2 (1:1000), phospho-specific PKB, phospho-specific p38 MAPK, phospho-specific JNK, and cleaved active caspase 3, GAPDH and TG2. Horseradish peroxidase-conjugated secondary antibodies (New England Biolabs (UK) Ltd), diluted 1:1000 in blocking buffer, were applied for 2 h at room temperature. Following removal of the unbound secondary antibody, blots were extensively washed and developed using the Enhanced Chemiluminescence (ECL) Detection System (Uptima, Interchim, France) and quantified by densitometry using Advanced Image Data Analysis Software (Fuji; version 3.52). Samples were also analysed using primary antibodies that recognise total ERK1/2, PKB, p38 MAPK and JNK (1:1000) in order to confirm the uniformity of protein loading.

## **2.7. Measurement of in situ TG2 activity**

H9c2 cells were seeded on 8-well chamber slides (15,000 cells/well) and cultured for 24 h in fully supplemented DMEM. The cells were then incubated for 6 h in medium containing 1 mM biotin-X-cadaverine (a cell permeable TG2 substrate; Perry et al., 1995) before experimentation. Where appropriate, cells were treated for 1 h with TG2 inhibitors Z-DON (150  $\mu\text{M}$ ) or R283 (200  $\mu\text{M}$ ) before the addition of 1  $\mu\text{M}$  formoterol. Following stimulation, cells were fixed with 3.7 % (w/v) paraformaldehyde and permeabilised with 0.1% (v/v) Triton™ X-100, both in PBS, for 15 min at room temperature. After washing, cells were blocked with 3% (w/v) BSA for 1 h at room temperature and the transglutaminase-

mediated biotin-X-cadaverine labelled protein substrates detected by incubation with FITC-conjugated ExtrAvidin® (1:200 v/v). Nuclei were stained with DAPI and images acquired using a Leica TCS SP5 II confocal microscope (Leica Microsystems, GmbH, Mannheim, Germany) equipped with a 20x air objective. Optical sections were typically 1-2 µm and the highest fluorescence intensity values were acquired and fluorescence intensity relative to DAPI stain quantified for each field of view. Image analysis and quantification were carried out using Leica LAS AF software.

## **2.8. Measurement of intracellular calcium**

H9c2 cells were plated in 24-well flat-bottomed plates (15,000 cells/well) and cultured for 24 h in fully supplemented DMEM. Cells were loaded with Fluo-8 AM (5 µM, 30-40 min) before mounting on the stage of a Leica TCS SP5 II confocal microscope (Leica Microsystems, GmbH, Mannheim, Germany) equipped with a 20x air objective. Cells were incubated at 37°C using a temperature controller and micro incubator (The Cube, Life Imaging Services, Basel, Switzerland) in the presence of imaging buffer (134 mM NaCl 134, 6 mM KCl 6, 1.3 mM CaCl<sub>2</sub> 1 mM MgCl<sub>2</sub> 1, 10 mM HEPES, and 10 mM glucose 10; pH 7.4). Using an excitation of 490 nm, emissions over 514 nm were collected. Cells were imaged and data collected every 1.7 s for 10 min. Increases in intracellular Ca<sup>2+</sup> were defined as  $F/F_0$  where  $F$  was the fluorescence at any given time, and  $F_0$  was the initial basal level of fluorescence.

## **2.9. Determination of TG2 phosphorylation**

Following stimulation, H9c2 cells were rinsed twice with 2.0 ml of chilled PBS and lysed with 500 µl of ice-cold lysis buffer (2 mM EDTA, 1.5 mM MgCl<sub>2</sub>, 10% (v/v) glycerol, 0.5% (v/v) IGEPAL, 0.1% (v/v) protease inhibitor cocktail, and 1% (v/v) phosphatase inhibitor cocktail 2 and 3 in PBS). Cell lysates were clarified by centrifugation (4°C for 10 min at 14000 x g), after which 500 µg of supernatant protein were incubated overnight at 4°C with 2 µg of

anti-TG2 monoclonal antibody or IgG. Immune complexes were precipitated using Pierce™ Classic Magnetic IP/Co-IP Kit (Fisher Scientific, Loughborough, UK). The precipitates were resolved by SDS-PAGE in 10% polyacrylamide gels, transferred to nitrocellulose membrane filters and probed using anti-phosphoserine or anti-phosphothreonine antibodies (1:1000). Antibody reactivity was visualised by ECL and quantified densitometrically, as described above.

### **2.10. Measurement of biotin-X-cadaverine incorporation into proteins serving as substrates for TG2**

Cellular proteins acting as substrates for endogenous TG2-catalysed polyamine incorporation reactions were investigated as described by Singh et al. (1995). Biotin-X-cadaverine labelled proteins were enriched using CaptAvidin™-agarose sedimentation beads (Life Technologies, Loughborough, UK), subjected to SDS-PAGE in 4-15% polyacrylamide gradient gels and separated proteins stained with Coomassie blue.

### **2.11. Proteomic analysis of TG2 biotin-X-cadaverine labelled substrate proteins**

Following pre-treatment with 1 mM biotin-X-cadaverine, H9c2 cells were treated with formoterol and lysed as described above. The proteins labelled with biotin-X-cadaverine were purified using CaptAvidin™-agarose and biotin-X-cadaverine labelled proteins were processed for trypsin digestion (Trypsin, proteomics grade; Sigma-Aldrich, UK).

Samples (~50 µg protein) were reduced and alkylated (1 µl 0.5 M DTT, 56° C for 20 min; 2.7 µl 0.55 M iodoacetamide, room temperature 15 min in the dark), dried in a vacuum concentrator (Eppendorf, UK) and resuspended in 100 µl 50 mM tri-ethyl ammonium bicarbonate (TEAB). Trypsin (2 µg in 2 µl of 1 mM HCl), was added in and incubated overnight at 37° C in a thermomixer. Samples were then evaporated to dryness in a vacuum concentrator and resuspended in 5% (v/v) acetonitrile/0.1% (v/v) formic acid (20 µl) and transferred to a HPLC vial for MS analysis. Samples (3 µl) were injected by

autosampler (Eksigent nanoLC 425 LC system) at 5  $\mu$ l/min directly onto a YMC Triart-C<sub>18</sub> column (25 cm, 3  $\mu$ m, 300  $\mu$ m i.d.) using gradient elution (2-40% Mobile phase B, followed by wash at 80% B and re-equilibration) over either 110 (120 min run time) min (for spectral library construction using data/information dependent acquisition DDA/IDA) or 50 min (60 min run time) for SWATH/DIA (Data Independent Acquisition) analysis (Gillet et al., 2012; Huang et al., 2015). Mobile phases consisted of A: 2% (v/v) acetonitrile, 5% (v/v) DMSO in 0.1% (v/v) formic acid; B: acetonitrile containing 5% (v/v) DMSO in 0.1% (v/v) formic acid.

A spectral library was constructed using the output from ProteinPilot 5 (SCIEX) combining four IDA runs per group (Control, formoterol treated), filtered, and aligned to spiked-in iRT peptides (Biognosys, Switzerland) using PeakView 2.2 (SCIEX) and the SWATH micro app 2.1 plug in. SWATH data extraction, quantitation and fold change analysis were carried out using SCIEX OneOmics cloud processing software (Lambert et al., 2013).

### **2.12. Data analysis**

All graphs and statistics (one-way ANOVA followed by Dunnett's multiple comparison test and two-way ANOVA for group comparison) were performed using GraphPad Prism<sup>®</sup> software (GraphPad 7.0 Software, Inc., USA). Agonist EC<sub>50</sub> values (concentration of agonist producing 50% of the maximal stimulation) were obtained by computer-assisted curve fitting using GraphPad Prism<sup>®</sup> software. Agonist p[EC<sub>50</sub>] values were subsequently calculated as the negative logarithm to base 10 of the EC<sub>50</sub>. Results represent mean  $\pm$  S.E.M. and *p* values <0.05 were considered statistically significant.

### **3. Results**

#### **3.1. Functional expression of the $\beta_2$ -adrenoceptor in H9c2 cells**

In this study the expression of mRNA encoding for  $\beta_1$ ,  $\beta_2$  and the  $\beta_3$ -adrenoceptors was determined in H9c2 cells by RT-PCR analysis. As shown in Fig. 1, mRNA was detected for all three  $\beta$ -adrenoceptor subtypes with a rank order of  $\beta_2 > \beta_1 = \beta_3$ . The selective  $\beta_2$ -adrenoceptor agonist formoterol ( $EC_{50} = 1.3 \pm 0.3$  nM;  $p[EC_{50}] = 8.9 \pm 0.1$ ;  $n=3$ ) stimulated a robust and pertussis toxin-insensitive increase in cAMP, confirming the functional expression of the  $\beta_2$ -adrenoceptor in H9c2 cells via  $G_s$ -protein coupling (Fig. 2A). Formoterol-induced cAMP responses were blocked by the non-selective  $\beta$ -adrenoceptor antagonist propranolol (1  $\mu$ M) and the selective  $\beta_2$ -adrenoceptor antagonist ICI 118,551 (1  $\mu$ M), whereas the selective  $\beta_1$ -adrenoceptor antagonist CGP 20712 (1  $\mu$ M) had no effect (Fig. 2B). Due to the lack of a selective  $\beta_1$ -adrenoceptor agonist, the functional expression of this subtype was assessed by determining the effect of the  $\beta_1$ -adrenoceptor antagonist CGP 20712 on dobutamine (non-selective  $\beta_1$  and  $\beta_2$  agonist)-induced cAMP accumulation. Dobutamine-induced cAMP responses were blocked by propranolol and ICI 118,551, whereas CGP 20712 had no effect (Fig. 2C). The selective  $\beta_3$ -adrenoceptor agonist CL 316243 (1  $\mu$ M) did not trigger a measureable increase in cAMP accumulation, suggesting that this subtype is not functionally expressed H9c2 cells (data not shown). Overall these data suggest functional expression of the  $\beta_2$ -adrenoceptor (and neither  $\beta_1$ - nor  $\beta_3$ -adrenoceptors) in H9c2 cells.

#### **3.2. Effect of $\beta_2$ -adrenoceptor activation on TG2-mediated biotin cadaverine amine incorporation and protein cross-linking activity**

Initial experiments investigated the effect of the  $\beta_2$ -adrenoceptor agonist formoterol on TG2 transamidase activity in H9c2 cardiomyoblasts. TG2 catalyses two types of transamidation, namely (i) intra-, and/or inter-molecular covalent cross-links between protein-bound

glutamine and lysine residues, and (ii) cross-links between small molecule primary amines and protein-bound glutamine (Nurminskaya and Belkin, 2012). H9c2 cells were treated with formoterol (100 nM) for varying times and cell lysates subjected to the biotin cadaverine amine-incorporation assay (Slaughter et al., 1992). Formoterol produced increases in TG2-catalysed biotin-cadaverine incorporation activity, peaking at 20 min (Fig. 3A). Furthermore, formoterol ( $EC_{50} = 15 \pm 2.3$  nM;  $p[EC_{50}] = 7.85 \pm 0.09$ ;  $n=4$ ; Fig. 3C) stimulated concentration-dependent increases in biotin-cadaverine incorporation activity. The effect of  $\beta_2$ -adrenoceptor activation on TG2-mediated protein cross-linking activity in H9c2 cells was also determined using the biotin-labeled peptide (biotin-TVQQEL) cross-linking assay (Trigwell et al., 2004). Formoterol (Fig. 3B) triggered time-dependent increases in TG2-mediated protein cross-linking activity peaking at 20 min. Formoterol ( $EC_{50} = 27 \pm 11$  nM;  $p[EC_{50}] = 7.69 \pm 0.15$ ;  $n=4$ ; Fig. 3D) also stimulated concentration-dependent increases in protein cross-linking activity. It is worth noting that levels of TG2 protein expression did not significantly change following stimulation with formoterol (data not shown). Although the  $\beta_2$ -adrenoceptor couples to  $G_s$  and  $G_i$  proteins (Daaka et al., 1997; Zamah et al., 2002), pre-treatment with pertussis toxin ( $G_{i/o}$ -protein blocker; 100 ng/ml) for 16 h had no significant effect on formoterol-induced TG2 activity (Fig. 3E and F). Finally, ICI 118,551 and propranolol blocked formoterol-induced TG2 activity (Fig. 4A and B).

### **3.3. The effect of TG2 inhibitors on $\beta_2$ -adrenoceptor-induced TG2 activity**

To confirm that TG2 is responsible for the  $\beta_2$ -adrenoceptor induced transglutaminase activity in H9c2 cardiomyocytes, two structurally different cell permeable TG2 specific inhibitors were tested; R283 (a small molecule; Freund et al., 1994) and Z-DON (peptide-based; Schaertl et al., 2010). Although these TG2 inhibitors are cell-permeable, inhibition of cellular TG2 is only achievable at concentrations significantly above their  $IC_{50}$  value versus purified enzyme (Schaertl et al., 2010; Freund et al., 1994). H9c2 cells were pre-treated for 1 h with Z-DON (150  $\mu$ M) or R283 (200  $\mu$ M) prior to stimulation with formoterol (1  $\mu$ M) for

20 min. Both inhibitors blocked formoterol-induced TG-mediated amine incorporation (Fig. 4C) and peptide cross-linking activity (Fig. 4D), confirming the involvement of TG2.

### **3.4. The role of Ca<sup>2+</sup> in $\beta_2$ -adrenoceptor- induced TG2 activity**

Since TG2 is a Ca<sup>2+</sup>-dependent enzyme we determined the role of Ca<sup>2+</sup> in  $\beta_2$ -adrenoceptor-induced TG2 activation. The role of extracellular Ca<sup>2+</sup> was assessed by measuring TG2 responses in the absence of extracellular Ca<sup>2+</sup> using nominally Ca<sup>2+</sup>-free Hanks/HEPES buffer containing 0.1 mM EGTA. Removal of extracellular Ca<sup>2+</sup> partially attenuated formoterol-induced TG2 activity (Fig. 4E and F). To assess the role of intracellular Ca<sup>2+</sup>, measurements of TG2 activation were also performed using cells pre-incubated with the Ca<sup>2+</sup> chelator BAPTA-AM (50  $\mu$ M for 30 min) in the absence of extracellular Ca<sup>2+</sup>. Loading cells with BAPTA in the absence of extracellular Ca<sup>2+</sup> did not lead to further inhibition of formoterol-induced TG2 activation (Fig. 4E and F). These observations suggest that  $\beta_2$ -adrenoceptor-induced TG2 activation is partially dependent upon the influx of extracellular Ca<sup>2+</sup>. We have previously measured A<sub>1</sub> adenosine receptor-induced changes in intracellular Ca<sup>2+</sup> in H9c2 cells using the fluorescent Ca<sup>2+</sup> indicator Fluo-8 (Vyas et al., 2016). In this study, formoterol did not trigger measurable increases in intracellular Ca<sup>2+</sup> in H9c2 cells loaded with Fluo-8 AM (data not shown).

### **3.5. The effect of protein and lipid kinase inhibitors on $\beta_2$ -adrenoceptor-induced TG2 activity**

Since the  $\beta_2$ -adrenoceptor activates PKA, the effect of two structurally different PKA inhibitors, *Rp*-cAMPs (de Wit et al., 1984) and KT-5720 (Kase et al., 1987), on formoterol-induced TG2 activity was assessed. Pre-treatment with *Rp*-cAMPs (50  $\mu$ M; Fig. 5A and B) and KT 5720 (5  $\mu$ M; Fig. 5C and D) partially attenuated formoterol-induced TG-mediated amine incorporation and protein cross-linking activity, suggesting the involvement of PKA. However, the effect of KT 5720 on protein cross-linking activity was not statistically

significant. Overall, these data indicate that PKA-dependent pathway(s) play a role in  $\beta_2$ -adrenoceptor-induced TG2 activity.

We have recently shown that the  $G_i$ -protein coupled  $A_1$  adenosine receptor stimulates TG2 activity in H9c2 cells via a number of protein kinases (e.g. PKC, ERK1/2, p38 MAPK and JNK1/2; Vyas et al., 2016). The  $\beta_2$ -adrenoceptor also triggers the activation of signalling cascades involving ERK1/2, p38 MAPK, JNK1/2 and PKB (Daaka et al., 1997; Okamoto et al., 1991; Steinberg, 1999; Yano et al., 2007). Modulation of ERK1/2, p38 MAPK, JNK1/2 and PKB activity following  $\beta_2$ -adrenoceptor activation was assessed in H9c2 cells by Western blotting using phospho-specific antibodies that recognise phosphorylated motifs within activated ERK1/2 (pTEpY), p38 MAPK (pTgPY), JNK1/2 (pTPpY) and PKB (pS<sup>473</sup>). Formoterol (1  $\mu$ M for 20 min) stimulated significant increases in ERK1/2 (Fig. 6) and PKB phosphorylation (data not shown for clarity) in H9c2 cells. In contrast, formoterol did not stimulate p38 MAPK or JNK1/2 activation (data not shown). As expected, pre-treatment with PD 98059 (50  $\mu$ M; MEK1 inhibitor) blocked formoterol-induced activation of ERK1/2 (Fig. 6A). Treatment with PD 98059 (50  $\mu$ M) also blocked formoterol-induced induced TG-mediated amine incorporation activity and protein cross-linking activity, suggesting a role for ERK1/2 in regulating these activities (Fig. 5E and F).

PI-3K plays a prominent up-stream role in  $\beta_2$ -adrenoceptor-induced modulation of ERK1/2 and PKB (Zhang et al., 2011). In this study the pan PI-3K inhibitors wortmannin (100 nM; Fig. 7A and B) and LY 294002 (30  $\mu$ M; Fig. 7C and D) blocked formoterol-induced TG2 activity. Furthermore, the selective PI-3K $\gamma$  inhibitor AS 605240 (1  $\mu$ M) also blocked formoterol-induced TG2 activity (Fig. 7E and F).

Given the role of ERK1/2, PI-3K and extracellular  $Ca^{2+}$  in formoterol-induced TG2 activation, we assessed whether PI-3K and extracellular  $Ca^{2+}$  play an up-stream role in ERK1/2 activation. Wortmannin, LY 294002, AS 605240 or removal of extracellular  $Ca^{2+}$  attenuated formoterol-induced ERK1/2 activation (Fig. 6). In contrast, *Rp*-cAMPs (Fig. 6B) and pertussis toxin (data not shown) had no significant effect on formoterol-induced ERK1/2

activation. These data suggest formoterol activates ERK1/2 via a PKA-independent but PI-3K and Ca<sup>2+</sup>-dependent pathway.

It is important to note that KT-5720, Rp-cAMPs, PD 98059, LY 294002, and AS 605240 had no significant effect on purified guinea pig liver TG2 activity (data not shown). Overall, these data suggest that TG2 activity is modulated in H9c2 cells by the  $\beta_2$ -adrenoceptor via a pathway involving PKA, ERK1/2 and PI-3K.

### **3.6. Visualisation of *in situ* TG2 activity following $\beta_2$ -adrenoceptor activation**

Biotin-X-cadaverine, a cell penetrating biotin-labelled primary amine, acts as the acyl-acceptor in intracellular TG2-mediated transamidating reactions and becomes incorporated into endogenous protein substrates of TG2, which can subsequently be visualised by reporters such as FITC- and HRP-ExtrAvidin<sup>®</sup> (Lee et al., 1993). H9c2 cells were pre-incubated with 1 mM biotin-X-cadaverine for 6 h at 37°C prior to treatment with formoterol for 1, 5, 10, 20, 30 and 40 min. After fixation and permeabilisation, intracellular proteins with covalently attached biotin-X-cadaverine were visualized using FITC-ExtrAvidin<sup>®</sup>. As shown in Fig. 8A, formoterol (100 nM) induced a time-dependent increase in the incorporation of biotin-X-cadaverine into endogenous protein substrates of TG2. These data are comparable to the time-dependent increases in TG2 activity observed *in vitro* (see Fig. 3). Formoterol-mediated biotin-X-cadaverine incorporation was also concentration-dependent ( $EC_{50} = 47 \pm 27$  nM;  $p[EC_{50}] = 7.65 \pm 0.27$ ;  $n=4$ ; Fig. 8B). To confirm the involvement of TG2 activation, cells were treated with the TG2 inhibitors Z-DON (150  $\mu$ M) and R283 (200  $\mu$ M) for 1 h prior to incubation with formoterol (1  $\mu$ M) for 20 min. Pre-treatment of cells with Z-DON and R283 resulted in the complete inhibition of formoterol-mediated biotin-X-cadaverine incorporation into protein substrates (Fig. 9A). The *in situ* responses to formoterol were attenuated by inhibitors of PKA (KT 5720 and Rp-cAMPs), PI-3K (LY 294002 and AS 605240) and MEK1 (PD 98059) and following removal of extracellular Ca<sup>2+</sup> (Fig. 9).

### **3.7. $\beta_2$ -adrenoceptor-induced TG2 phosphorylation**

The effect of formoterol on TG2 phosphorylation was examined via immunoprecipitation of TG2, followed by SDS-PAGE and Western blot analysis using anti-phosphoserine and anti-phosphothreonine antibodies. As shown in Fig. 10, formoterol (1  $\mu$ M) enhanced TG2-bound phosphoserine and phosphothreonine. Pre-treatment with *Rp*-cAMPs (50  $\mu$ M), PD 98059 (50  $\mu$ M) and AS 605240 (1  $\mu$ M) attenuated formoterol-induced TG2 phosphorylation (Fig. 10 and 11). Finally, removal of extracellular  $\text{Ca}^{2+}$  attenuated formoterol-induced TG2 activity (Fig. 11). Formoterol-induced increases in TG2 phosphorylation were also blocked by the pan PI-3K inhibitors wortmannin and LY 294002 (data not shown).

### **3.8. Identification of biotin-X-cadaverine labelled protein substrates**

Following stimulation with formoterol (1  $\mu$ M for 20 min), cell extracts from biotin-X-cadaverine labelled cells were enriched using CaptAvidin<sup>™</sup>-agarose sedimentation beads, resolved by SDS-PAGE on 4-15% polyacrylamide gradient gels and visualised using Coomassie blue stain (Fig. 12). As shown in Fig. 12A, the intensity of some proteins bands eluted from the CaptAvidin<sup>™</sup>-agarose beads increased following stimulation with formoterol (1  $\mu$ M) which may be indicative of TG2-mediated transamidation and/or altered interactions with TG2 substrate binding partners. Furthermore, pre-treatment with Z-DON and R283 attenuated the levels of eluted proteins (Fig. 12). However, it is notable that the intensity of several protein bands also decreased following formoterol treatment, indicative of reduced levels of transamidation and/or altered interactions with TG2 substrate binding partners. To identify the proteins captured and eluted from CaptAvidin<sup>™</sup>-agarose beads, eluates were analysed by SWATH-MS (Sequential Windowed Acquisition of All Theoretical Fragment Ion Mass Spectra; Huang et al., 2015). This technique allows quantification of mass spectrometry data and the results presented are shown as formoterol-induced fold-changes in proteins eluted from CaptAvidin<sup>™</sup>-agarose compared to control unstimulated cells. SWATH analysis revealed increases in eight proteins not previously identified as TG2 protein

substrates and five known substrates in response to  $\beta_2$ -adrenoceptor activation in H9c2 cells (Table 1). Interestingly, SWATH-MS analysis also identified proteins whose profile revealed a decrease in formoterol treated cells when compared to untreated control cells (Table 1). Further work is needed to determine whether these changes represent altered transamidation and/or interactions with TG2 substrate binding partners.

## **4. Discussion**

In this study, we have established for the first time that the  $\beta_2$ -adrenoceptor triggers robust increases in TG2 transamidation activity in H9c2 cells via a signalling pathway dependent upon PKA, ERK1/2, PI-3K and extracellular  $\text{Ca}^{2+}$ .

### ***4.1. In vitro modulation of TG2 by the $\beta_2$ -adrenoceptor***

Activation of the  $\beta_2$ -adrenoceptor with formoterol triggered time- and concentration-dependent increases in the amine incorporating and protein cross-linking activity of TG2. It is notable that the potency in mediating biotin-cadaverine incorporation and protein cross-linking is lower than for formoterol-stimulated cAMP accumulation. These differences may be a consequence of biased agonism between agonist-induced cAMP accumulation versus TG2 activation (Rajagopal et al., 2011). Alternatively, it may be a consequence of the multiple signalling pathways e.g. PKA, ERK1/2, PI-3K, and  $\text{Ca}^{2+}$  shown to be required for TG2 modulation.

### ***4.2. Role of extracellular $\text{Ca}^{2+}$ in $\beta_2$ -adrenoceptor-induced TG2 activation***

Since the transamidating activity of TG2 is dependent upon  $\text{Ca}^{2+}$ , we assessed the role of extracellular and intracellular  $\text{Ca}^{2+}$  in  $\beta_2$ -adrenoceptor-induced TG2 activation. Removal of extracellular  $\text{Ca}^{2+}$  partially inhibited formoterol-induced TG2-mediated transamidation activity. Surprisingly, formoterol did not trigger observable increases in intracellular  $[\text{Ca}^{2+}]$  in H9c2 cells loaded with Fluo-8 AM. At present the reason(s) for this discrepancy are unclear but it may reflect very localized formoterol-induced increases in intracellular  $[\text{Ca}^{2+}]$  (as a consequence of  $\text{Ca}^{2+}$  influx) that, whilst sufficient to trigger TG2 activation, were not detectable using the methodology employed. It is important to note that, although changes in intracellular  $[\text{Ca}^{2+}]$  required for TG2 activation are typically in the order 3-100  $\mu\text{M}$ , there is growing evidence that intracellular  $[\text{Ca}^{2+}]$  can reach levels sufficient to activate TG2 (Király et al., 2011). Alternatively, the role of  $\text{Ca}^{2+}$  in formoterol-induced TG2 activation

may be in the sensitization of TG2 to  $\beta_2$ -adrenoceptor-mediated activation. For example, interaction of TG2 with protein binding partners and/or membrane lipids have been proposed to induce a conformational change that promotes activation at low levels of intracellular  $[Ca^{2+}]$  (Király et al., 2011). Clearly, further studies are required to determine precisely how  $\beta_2$ -adrenoceptor-induced TG2 activation occurs in the absence of detectable increases in intracellular  $Ca^{2+}$ , but the kinase-dependent pathways outlined in the present study could be central to these novel aspects of TG2 regulation.

#### **4.3. Role of PKA and ERK1/2 in $\beta_2$ -adrenoceptor-induced TG2 activation**

The role of PKA and other protein/lipid kinases in formoterol-induced TG2 activation was explored using appropriate pharmacological inhibitors. The PKA inhibitors *Rp*-cAMPs and KT 5720 attenuated formoterol-induced TG2 responses, suggesting a role for PKA. The MEK1/2 (up-stream activator of ERK1/2) inhibitor PD 98059 also attenuated formoterol-induced TG2 activation. These data are in agreement with the role of ERK1/2 in TG2 activation triggered by the  $G_i$ -protein coupled  $A_1$  adenosine receptor (Vyas et al., 2016). The attenuation of formoterol-induced TG2 responses by *Rp*-cAMPs and KT 5720 may be a consequence of the up-stream role of PKA in  $\beta_2$ -adrenoceptor-induced ERK1/2 activation (Schmitt and Stork, 2000). However, in H9c2 cells formoterol-induced ERK1/2 activation was insensitive to PKA inhibition and therefore the role of PKA in TG2 activation appears to be independent of ERK1/2. However, removal of extracellular  $Ca^{2+}$  and inhibition of PI-3K attenuated formoterol-induced ERK1/2 activation. Although beyond the scope of the present study, it would be of interest to investigate further the mechanism(s) underlying  $\beta_2$ -adrenoceptor - induced ERK1/2 activation in H9c2 cells.

PI-3K plays a prominent role in  $\beta_2$ -adrenoceptor signalling (Zhang et al., 2011). In the present study we have shown that formoterol-induced TG2 activity is sensitive to the pan PI-3K inhibitors wortmannin and LY 294002 and the selective PI-3K $\gamma$  inhibitor AS 605240.

Overall, these observations suggest that PI-3K lies up-stream of ERK1/2 stimulation and TG2 activation in H9c2 cells.

#### **4.4. $\beta_2$ -adrenoceptor-induced phosphorylation of TG2**

Given the apparent role of PKA and ERK1/2 in the regulation of TG2, we investigated the phosphorylation status of TG2 following  $\beta_2$ -adrenoceptor stimulation. The data obtained demonstrate that TG2 is phosphorylated in response to  $\beta_2$ -adrenoceptor activation. However, it is important to state that the relationship between formoterol-induced TG2 phosphorylation and TG2 transamidase activity is not known. Further work is required to determine if formoterol stimulated TG2 activation is dependent upon formoterol-induced TG2 phosphorylation. It is notable that we have recently reported that TG2 is also phosphorylated following stimulation of the A<sub>1</sub> adenosine receptor in H9c2 cells (Vyas et al., 2016). Hence, the modulation of TG2 phosphorylation may represent a common downstream target of GPCR signalling. Previous studies have shown that TG2 is phosphorylated by PKA at Ser<sup>215</sup> and Ser<sup>216</sup> (Mishra and Murphy, 2006). At present it is not known if formoterol triggers TG2 phosphorylation at Ser<sup>215</sup> and Ser<sup>216</sup>. However, previous studies have revealed that PKA-mediated phosphorylation of TG2 at these sites has several potential consequences, including promotion of protein-protein interactions, enhancement of TG2 kinase activity and inhibition of transamidating activity (Mishra and Murphy, 2006; Mishra et al., 2007). In this study  $\beta_2$ -adrenoceptor-induced PKA activation promoted TG2 transamidating activity. The attenuation of *in vitro* TG2 cross-linking activity by PKA observed by Mishra *et al.* (2007) was achieved using histidine-tagged TG2 immobilized on nickel-agarose and incubation with purified PKA. Hence, *in vivo* regulation of TG2 activity by PKA may be influenced by interaction of TG2 with other proteins and/or lipids. Thus, further studies are warranted in order to determine the consequence(s) of  $\beta_2$ -adrenoceptor-induced TG2 phosphorylation. In view of the multiple protein/lipid kinases (PKA, ERK1/2, PI-3K) implicated in  $\beta_2$ -adrenoceptor-induced TG2 activation, we investigated the influence of

kinase inhibitors on TG2 phosphorylation. Formoterol-induced increases in TG2 phosphorylation were reduced following pharmacological inhibition of PKA, MEK1/2, PI-3K and removal of extracellular  $\text{Ca}^{2+}$ . Whilst the attenuation of TG2 phosphorylation following PI-3K inhibition is most likely due to the upstream role of PI-3K in ERK1/2 activation, it is conceivable that the protein kinase activity of PI-3K may directly phosphorylate TG2 (Hunter 1995; Naga Prasad et al., 2005). Further studies are required to establish if PKA, ERK1/2 or indeed PI-3K directly catalyse the phosphorylation of TG2. Finally, removal of extracellular  $\text{Ca}^{2+}$  attenuated formoterol-induced TG2 phosphorylation. These data may reflect the role of extracellular  $\text{Ca}^{2+}$  in formoterol-induced ERK1/2 activation. Alternatively, it may be that conformational changes in TG2 triggered by  $\text{Ca}^{2+}$  facilitate its subsequent phosphorylation by PKA and/or ERK1/2. Conversely, it is also a possibility that TG2 phosphorylation may sensitize TG2 to activation in the presence of low  $\text{Ca}^{2+}$  as discussed above. Further work to identify the phosphorylation site(s) targeted following  $\beta_2$ -adrenoceptor activation would be worthwhile.

#### ***4.5. In situ $\beta_2$ -adrenoceptor-induced polyamine incorporation into protein substrates***

Intracellular polyamines e.g. spermine, spermidine, and putrescine can be covalently attached onto proteins via TG2-mediated transamidation activity, resulting in the incorporation of a positively charged group into the target protein. Thus, TG2-mediated polyamination may promote changes in protein conformation, which could lead to alterations in protein function (Yu et al., 2015). For example, the TG2-mediated incorporation of polyamines into RhoA results in constitutive G-protein activity (Makitie et al., 2009; Shin et al., 2008; Singh et al., 2001), whereas the incorporation of polyamines into phospholipase  $A_2$  results in a 2-3 fold increase in enzymic activity (Cordella-Miele et al., 1993). In the current study, *in situ* TG2 activity increased following stimulation of the  $\beta_2$ -adrenoceptor. These *in situ* responses were comparable to amine incorporation activity

observed *in vitro* and were also sensitive to pharmacological inhibition of PKA, MEK1/2, PI-3K and removal of extracellular  $\text{Ca}^{2+}$ , confirming the role of these signalling pathways in  $\beta_2$ -adrenoceptor-induced TG2 activation. It is interesting to speculate that  $\beta_2$ -adrenoceptor-mediated incorporation of polyamines might regulate the function of a range of cellular targets and may represent a new paradigm in  $\beta_2$ -adrenoceptor signaling and regulation of cellular function.

#### **4.6. Identification of proteins in CaptAvidin™-agarose bead eluates**

SWATH™-MS analysis identified eight proteins not previously identified as TG2 protein substrates (e.g. Protein S100-A6) and five known substrates (Table 1) in response to formoterol stimulation. It is beyond the scope of the present discussion to describe the biological functions/roles of all of these proteins but it is interesting to note that protein S100-A6 is a  $\text{Ca}^{2+}$  binding protein that is known to interact with tropomyosin and actin (Donato et al., 2013), and that several other identified proteins are cytoskeletal proteins (e.g. actin, myosin, tropomyosin). Hence it is conceivable that TG2-mediated modulation of protein S100-A6 function plays a role in  $\beta_2$ -adrenoceptor-induced regulation of cardiomyocyte contractility. Interestingly, recent studies have shown that TG2 plays a role in oxytocin-induced contraction of human myometrium (Alcock et al., 2011).

Further interrogation of the SWATH data identified a large number of proteins (including many whose function is linked with muscle contraction) that displayed a pronounced decrease following treatment with formoterol indicative of altered levels of transamidation of specific substrates and/or proteins interacting with them (Table 1). It is notable that TG2 can catalyse simultaneous transamidation and deamidation of heat shock protein 20 and thus  $\beta_2$ -adrenoceptor-induced activation may also promote the deamidation of TG2 substrates (Boros et al., 2006). Overall, these data have identified a large number of proteins whose elution profile from CaptAvidin™-agarose beads changes markedly in

formoterol treated cells. The challenge for future work will be to explore the role of such TG2-mediated modifications in  $\beta_2$ -adrenoceptor function and signalling.

At present very little is known of the *in vivo* regulation of TG2 in cardiomyocytes and how such activity may alter under pathological conditions. Interestingly, TG2 knockout mice display no significant change in haemodynamic parameters (heart rate, systolic and diastolic blood pressure and contractility) when compared to non-transgenic animals (Nanda et al., 2001). These observations suggest no significant role for TG2 in normal cardiovascular function. More recent studies have demonstrated that TG2 mediates cell survival against ischaemia/reperfusion injury by regulating ATP synthesis in cardiomyocytes derived from TG2<sup>-/-</sup> knockout mice, suggesting a cardioprotective role for TG2 (Szondy et al., 2006). Interestingly, increased levels of TG2 expression have been demonstrated in animal models of cardiac hypertrophy (Iwai et al., 1995) and from heart failure patients (Hwang et al., 1996). Furthermore, cardiac-specific over-expression of TG2 is associated with cardiac hypertrophy, apoptosis and fibrosis (Small et al., 1999; Zhang et al., 2003). Overall, these studies demonstrate a potential role for TG2 in cardiac pathology (Iismaa et al., 2009). Regarding the increased levels of TG2 observed in heart failure patients it is interesting to speculate that TG2 activation, as a consequence of the elevated levels of catecholamines associated with heart failure, may contribute to the pathophysiology of heart failure. Alternatively, TG2 activation under these conditions may play a protective role during heart failure.

In conclusion, our data have revealed for the first time that activation of TG2 occurs by the  $\beta_2$ -adrenoceptor via a multi-protein kinase pathway. Work is currently underway to explore further the function(s) of  $\beta_2$ -adrenoceptor-induced TG2 activity in cardiomyocytes.

### **Conflict of interest**

None declared

## **Acknowledgements**

We would like to thank Gordon Arnott for helping with confocal imaging.

## Figure legends

**Fig. 1.**  $\beta$ -adrenoceptor mRNA expression in H9c2 cells. mRNA isolated from H9c2 cells was subjected to RT-PCR using intron spanning  $\beta_1$ ,  $\beta_2$  and  $\beta_3$ -adrenoceptor gene specific primers. mRNA samples isolated from rat heart ( $\beta_1$ -adrenoceptor) and rat lung ( $\beta_2$  and  $\beta_3$ -adrenoceptor) were used as positive controls. L: 100 bp DNA standard; lane 1: no DNA control; lanes 2, 4 and 6: positive control; lanes 3, 5 and 7: H9c2 cell-derived mRNA. mRNA control using GAPDH primers is shown in the lower panel. The results presented are representative of three independent experiments.

**Fig. 2.**  $\beta$ -adrenoceptor agonist-induced cAMP accumulation in H9c2 cells. Where indicated cells were pre-treated for 16 h with 100 ng/ml pertussis toxin. Cells were either (A) treated with the indicated concentrations of formoterol for 20 min; (B) pretreated for 30 min with propranolol (100 nM), CGP 20712 (100 nM), or ICI 118551 (100 nM) prior to 20 min stimulation with formoterol (10 nM) or (C) pretreated for 30 min with propranolol (100 nM), CGP 20712 (100 nM), or ICI 118551 (100 nM) prior to 20 min stimulation with dobutamine (1  $\mu$ M). Levels of cAMP were determined as described in Materials and Methods. Data are presented as levels of cAMP in nM. The results represent the mean  $\pm$  S.E.M. of four experiments each performed in triplicate. \* $P$ <0.05, \*\* $P$ <0.01, \*\*\* $P$ <0.001, and \*\*\*\* $P$ <0.0001, (a) versus control and (b) versus 10 nM formoterol or 1  $\mu$ M dobutamine alone.

**Fig. 3.** Effect of the  $\beta_2$ -adrenoceptor agonist formoterol on TG2 activity in H9c2 cells. Cells were stimulated with formoterol (100 nM) for the indicated time periods (panels A and C). Concentration-response curves for formoterol in cells treated with agonist for 20 min (panels B and D). Where indicated H9c2 cells were pre-treated for 16 h with 100 ng/ml

pertussis toxin prior to 20 min stimulation with 1  $\mu$ M formoterol (panels E and F). Cell lysates were subjected to the biotin-cadaverine incorporation (panels A, C and E) or the peptide cross-linking assay (panels B, D and F). Data points represent the mean  $\pm$  S.E.M. for TG2 specific activity from four independent experiments. \* $P$ <0.05, \*\* $P$ <0.01, \*\*\* $P$ <0.001 and \*\*\*\* $P$ <0.0001, (a) *versus* control response and (b) versus 1  $\mu$ M formoterol alone.

**Fig. 4.** Effect of  $\beta$ -adrenoceptor antagonists, inhibitors of TG2 and removal of extracellular  $\text{Ca}^{2+}$  on formoterol-induced TG2 activity in H9c2 cells. H9c2 cells were pretreated for 30 min with the antagonists ICI 118,551 (1  $\mu$ M;  $\beta_2$ -adrenoceptor selective) and propranolol (1  $\mu$ M non-selective  $\beta$ -adrenoceptor) or for 1 h with the TG2 inhibitors Z-DON (150  $\mu$ M) and R283 (200  $\mu$ M) prior to stimulation with formoterol (1  $\mu$ M; 20 min). H9c2 cells were also stimulated for 20 min with formoterol (1  $\mu$ M) either in the presence of extracellular  $\text{Ca}^{2+}$  (1.8 mM) or in its absence using nominally  $\text{Ca}^{2+}$ -free Hanks/HEPES buffer containing 0.1 mM EGTA. Experiments were also performed using cells pre-incubated for 30 min with 50  $\mu$ M BAPTA/AM and in the absence of extracellular  $\text{Ca}^{2+}$  (nominally  $\text{Ca}^{2+}$ -free Hanks/HEPES buffer containing 0.1 mM EGTA) to chelate intracellular  $\text{Ca}^{2+}$ . Cell lysates were subjected to biotin-cadaverine incorporation assay (panels A, C and E) or peptide cross-linking assay (panels B, D and F). Data points represent the mean  $\pm$  S.E.M. for TG2 specific activity from four independent experiments. \* $P$ <0.05, \*\* $P$ <0.01, \*\*\* $P$ <0.001 and \*\*\*\* $P$ <0.0001, (a) versus control and (b) versus 1  $\mu$ M formoterol in the presence of extracellular  $\text{Ca}^{2+}$ .

**Fig. 5.** Effect of PKA and ERK1/2 inhibition on formoterol-induced TG2 activity. H9c2 cells were pretreated for 30 min with *Rp*-cAMPs (50  $\mu$ M), KT-5720 (5  $\mu$ M) or PD 98059 (50  $\mu$ M) prior to 20 min stimulation with formoterol (1  $\mu$ M). Cell lysates were subjected to biotin-cadaverine incorporation (panels A, C and E) or peptide cross-linking assays (panels B, D

and F). Data points represent the mean  $\pm$  S.E.M. for TG2 specific activity from four independent experiments. \* $P$ <0.05, \*\* $P$ <0.01, \*\*\* $P$ <0.001 and \*\*\*\* $P$ <0.0001, (a) versus control and (b) versus 1  $\mu$ M formoterol alone.

**Fig. 6.** Effect of formoterol on ERK1/2 phosphorylation in H9c2 cells. Where indicated, H9c2 cells were pre-treated for 30 min with A) PD 98059 (50  $\mu$ M), B) *Rp*-cAMPs (50  $\mu$ M), C) wortmannin (100 nM), D) LY 294002 (30  $\mu$ M), or E) AS 605240 (1  $\mu$ M) prior to stimulation with formoterol (1  $\mu$ M) for 20 min. In Panel (F) cells were stimulated for 20 min with formoterol (1  $\mu$ M) either in the presence of extracellular  $\text{Ca}^{2+}$  (1.3 mM) or in its absence using nominally  $\text{Ca}^{2+}$ -free Hanks/HEPES buffer containing 0.1 mM EGTA. Cell lysates were analysed by Western blotting for activation of ERK1/2 using phospho-specific antibodies. Samples were subsequently analysed on separate blots using antibodies that recognize total ERK1/2 (data omitted for clarity). Data are expressed as the percentage of values for control cells (=100%) in the absence of protein kinase inhibitor and represent the mean  $\pm$  S.E.M. of four independent experiments. \*\* $P$ <0.01 and \*\*\* $P$ <0.001, (a) versus control and (b) versus 1  $\mu$ M formoterol alone.

**Fig. 7.** Effect of PI-3K inhibitors on formoterol -induced TG2 activity. H9c2 cells were pretreated for 30 min with wortmannin (100 nM), LY 294002 (30  $\mu$ M), or AS 605240 (1  $\mu$ M) prior to 20 min stimulation with formoterol (1  $\mu$ M). Cell lysates were subjected to protein biotin-cadaverine amine incorporation assay (panels A, C and E) or cross-linking assay (panels B, D and F). Data points represent the mean  $\pm$  S.E.M. TG2 specific activity from four independent experiments. \* $P$ <0.05, \*\* $P$ <0.01 and \*\*\* $P$ <0.001, (a) versus control and (b) versus 1  $\mu$ M formoterol alone.

**Fig. 8.** Formoterol-induced *in situ* TG2 activity in H9c2 cells. Cells were incubated with 1 mM biotin-X-cadaverine (BTC) for 6 h, after which they were treated with (A) 100 nM

formoterol for 1, 5, 10, 20, 30 or 40 min or (B) the indicated concentrations (in M) of formoterol for 20 min. TG2-mediated biotin-X-cadaverine incorporation into intracellular proteins was visualized using FITC-ExtrAvidin<sup>®</sup> (green). Nuclei were stained with DAPI (blue) and viewed using a Leica TCS SP5 II confocal microscope (20x objective lens). Images presented are from one experiment and representative of three independent experiments. Quantified data points for (C) time course and (D) concentration-response curve experiments represent the mean  $\pm$  S.E.M. of fluorescence intensity relative to DAPI stain for five fields of view each from three to four independent experiments. \* $P$ <0.05, \*\* $P$ <0.01, \*\*\* $P$ <0.001 and \*\*\*\* $P$ <0.0001 versus control response.

**Fig. 9.** Effects of TG2 and kinase inhibitors on *in situ* TG2 activity in H9c2 cells following stimulation with formoterol. Cells were incubated with 1 mM biotin-X-cadaverine (BTC) for 6 h after which they were treated as follows: (A) 1 h with the TG2 inhibitors Z-DON (150  $\mu$ M) or R283 (200  $\mu$ M), (B) 30 min with KT 5720 (5  $\mu$ M) or *Rp*-cAMPs (50  $\mu$ M), (C) 30 min with PD 98059 (50  $\mu$ M) or LY 294002 (30  $\mu$ M) or (D) 30 min with AS 605240 (1  $\mu$ M) or in the absence of extracellular Ca<sup>2+</sup> for 30 min (nominally Ca<sup>2+</sup>-free Hanks/HEPES buffer containing 0.1 mM EGTA), prior to 20 min stimulation with formoterol (1  $\mu$ M). TG2-mediated biotin-X-cadaverine incorporation into intracellular proteins was visualized using FITC-ExtrAvidin<sup>®</sup> (green). Nuclei were stained with DAPI (blue) and viewed using a Leica TCS SP5 II confocal microscope (20x objective lens). Images presented are from one experiment and are representative of three independent experiments. Quantified data points represent the mean  $\pm$  S.E.M. of fluorescence intensity relative to DAPI stain for five fields of view each from three independent experiments. \* $P$ <0.05, \*\* $P$ <0.01, \*\*\* $P$ <0.001 and \*\*\*\* $P$ <0.0001, (a) versus control and (b) versus 1  $\mu$ M formoterol alone.

**Fig. 10.** Effect of PKA and ERK1/2 inhibition on formoterol-induced phosphorylation of TG2. Where indicated, H9c2 cells were incubated for 30 min with *Rp*-cAMPs (50  $\mu$ M) or PD 98059

(50  $\mu\text{M}$ ) prior to stimulation with formoterol (1  $\mu\text{M}$ ) for 20 min. Following stimulation, cell lysates were subjected to immunoprecipitation using anti-TG2 monoclonal antibody as described under "Materials and Methods". The resultant immunoprecipitated protein(s) were subjected to SDS-PAGE and analysed via Western blotting using (A) anti-phosphoserine and (B) anti-phosphothreonine antibodies. One tenth of the input was added to the first lane to show the presence of phosphorylated proteins prior to immunoprecipitation and negative controls with the immunoprecipitation performed with beads or IgG only were included to demonstrate the specificity of the bands shown. Quantified data for formoterol-induced increases in TG2-associated serine and threonine phosphorylation are expressed as a percentage of that observed in control cells (100%). Data points represent the mean  $\pm$  S.E.M. from three independent experiments. \* $P < 0.05$ , \*\* $P < 0.01$  and \*\*\* $P < 0.001$  (a) versus control and (b) versus formoterol alone.

**Fig. 11.** Roles of extracellular  $\text{Ca}^{2+}$  and PI-3K in formoterol-induced phosphorylation of TG2. Measurements of formoterol-induced TG2 phosphorylation were performed either in the absence of extracellular  $\text{Ca}^{2+}$  using nominally  $\text{Ca}^{2+}$ -free Hanks/HEPES buffer containing 0.1 mM EGTA, as indicated, or in cells incubated for 30 min with AS 60540 (1  $\mu\text{M}$ ) prior to stimulation with formoterol (1  $\mu\text{M}$ ) for 20 min. Following stimulation, cell lysates were subjected to immunoprecipitation using anti-TG2 monoclonal antibody as described under "Materials and Methods". The resultant immunoprecipitated protein(s) were subjected to SDS-PAGE and Western blot analysis using (A) anti-phosphoserine and (B) anti-phosphothreonine antibodies. One tenth of the input was added to the first lane to show the presence of phosphorylated proteins prior to immunoprecipitation and negative controls with the immunoprecipitation performed with beads or IgG only were included to demonstrate the specificity of the bands shown. Quantified data for formoterol-induced increases in TG2-associated serine and threonine phosphorylation are expressed as a percentage of that observed in control cells (100%). Data points represent the mean  $\pm$  S.E.M. from three

independent experiments.  $*P<0.05$  and  $**P<0.01$  (a) versus control and (b) versus formoterol alone.

**Fig. 12.** Detection of *in situ* TG2 activity and protein substrates in formoterol-treated H9c2 cells. Cells were incubated with 1 mM biotin-X-cadaverine for 6 h, after which they were treated for 1 h with the TG2 inhibitors Z-DON (150  $\mu$ M) or R283 (200  $\mu$ M) before stimulation with formoterol (1  $\mu$ M) for 20 min. Biotin-X-cadaverine-labelled proteins were enriched using CaptAvidin™ agarose sedimentation beads and eluted proteins subjected to SDS-PAGE on 4-15% polyacrylamide gradient gels. (A) Coomassie blue staining of enriched biotin-X-cadaverine-labelled proteins following SDS-PAGE. (B) Quantification of protein substrates detected using Coomassie blue staining. Densitometry of each lane (total protein) was carried out using Advanced Image Data Analyser software (Fuji; version 3.52) and data are expressed as a percentage of basal TG2 protein substrate levels. Values are means  $\pm$  S.E.M. from three independent experiments.  $***P<0.001$  and  $****P<0.0001$ , (a) versus control response, (b) versus formoterol alone.

**Table 1.** Identification of proteins showing increased or decreased levels in eluates from CaptAvidin™-agarose columns following formoterol-induced  $\beta_2$ -adrenoceptor activation.

<b>Protein Name</b>	<b>Uniprot Accession</b>	<b>Uniprot Name</b>	<b>Absolute Fold Change*</b>
<b>Formoterol-induced increases</b>			
<sup>d</sup> Collagen alpha-1(I) chain	P02454	CO1A1_RAT	2.64
<sup>a</sup> Protein S100-A6	P05964	S10A6_RAT	2.45
<sup>d</sup> Collagen alpha-1(III) chain	P13941	CO3A1_RAT	2.39
<sup>f</sup> Protein SET	Q63945	SET_RAT	2.26
<sup>b</sup> L-lactate dehydrogenase A chain	P04642	LDHA_RAT	1.95
<sup>f</sup> Annexin A5	P14668	ANXA5_RAT	1.91
<sup>d</sup> Collagen alpha-2(I) chain	P02466	CO1A2_RAT	1.86
<sup>b</sup> Malate dehydrogenase, mitochondrial	P04636	MDHM_RAT	1.84
<sup>b</sup> D-3-phosphoglycerate dehydrogenase	O08651	SERA_RAT	1.65
<sup>f</sup> Galectin-1	P11762	LEG1_RAT	1.62
<sup>c</sup> Ribonuclease inhibitor	P29315	RINI_RAT	1.57
<sup>c</sup> Histone H1.5	D3ZBN0	H15_RAT	1.46
<sup>d</sup> 60S ribosomal protein L7	P05426	RL7_RAT	1.32
<b>Formoterol-induced decreases</b>			
<sup>d</sup> Calumenin	O35783	CALU_RAT	-3.27
<sup>d</sup> EH domain-containing protein 2	Q4V8H8	EHD2_RAT	-2.76
<sup>b</sup> Myosin regulatory light polypeptide 9	Q64122	MYL9_RAT	-2.66
<sup>c</sup> Cysteine and glycine-rich protein 1	P47875	CSRP1_RAT	-2.46
<sup>d</sup> Dynactin subunit 2	Q6AYH5	DCTN2_RAT	-2.40
<sup>b</sup> Actin, gamma-enteric smooth muscle	P63269	ACTH_RAT	-2.36
<sup>c</sup> Transcription intermediary factor 1-beta	O08629	TIF1B_RAT	-2.11
<sup>e</sup> Lactadherin	P70490	MFGM_RAT	-2.07
<sup>d</sup> Dynactin subunit 1	P28023	DCTN1_RAT	-2.03
<sup>a</sup> Four and a half LIM domains protein 1	Q9WUH4	FHL1_RAT	-1.89
<sup>b</sup> Myosin light polypeptide 6	Q64119	MYL6_RAT	-1.84
<sup>b</sup> Filamin-C	D3ZHA0	FLNC_RAT	-1.80
<sup>b</sup> Myosin-9	Q62812	MYH9_RAT	-1.73
<sup>f</sup> PDZ and LIM domain protein 7	Q9Z1Z9	PDLI7_RAT	-1.72
<sup>d</sup> Alpha-centractin	P85515	ACTZ_RAT	-1.72
<sup>a</sup> Integrin beta-1	P49134	ITB1_RAT	-1.70
<sup>b</sup> Tropomyosin alpha-1 chain	P04692	TPM1_RAT	-1.68
<sup>a</sup> Transforming growth factor beta-1-induced transcript 1 protein	Q99PD6	TGFI1_RAT	-1.65
<sup>a</sup> Rho-associated protein kinase 2	Q62868	ROCK2_RAT	-1.60
<sup>d</sup> Ras-related protein Rab-7a	P09527	RAB7A_RAT	-1.53
<sup>g</sup> Heat shock protein HSP 90-alpha	P82995	HS90A_RAT	-1.53
<sup>b</sup> LIM and SH3 domain protein 1	Q99MZ8	LASP1_RAT	-1.43
<sup>b</sup> Myosin regulatory light chain RLC-A	P13832	MRLCA_RAT	-1.43
<sup>f</sup> 14-3-3 protein theta	P68255	1433T_RAT	-1.41
<sup>g</sup> Endoplasmic (Heat shock protein HSP 90-beta 1)	Q66HD0	ENPL_RAT	-1.38

H9c2 cells were pre-incubated with biotin-X-cadaverine prior to treatment with formoterol (1  $\mu$ M) and biotin-cadaverine labelled proteins were captured and analysed by SWATH MS. \*Absolute fold changes in formoterol treated samples versus control (n=4) were calculated using SCIEX OneOmics with parameters MLR weight > 0.15, confidence >70%, algorithms used described by Lambert *et al.*, (2013). Known TG2 targets appearing in the TG2 substrate database (Csósz *et al.*, 2009) or identified by Yu *et al.* (2015) and Almami *et al.* (2014) are indicated in *italics*. Proteins are grouped according to their functions and/or cellular function as follows: <sup>a</sup>cell signalling; <sup>b</sup>metabolism; <sup>c</sup>transcription/translation; <sup>d</sup>vesicular trafficking/extracellular matrix constituent; <sup>e</sup>apoptosis; <sup>f</sup>structural/scaffolding protein; <sup>g</sup>protein folding.

## References

Agnihotri N, Mehta K (2017) Transglutaminase-2: evolution from pedestrian protein to a promising therapeutic target. *Amino Acids* 49: 425-439.

Alcock J, Warren AY, Goodson YJ, Hill SJ, Khan RN, Lymn JS (2011) Inhibition of tissue transglutaminase 2 attenuates contractility of pregnant human myometrium. *Biol Reprod* 84: 646-653.

Almami I, Dickenson JM, Hargreaves AJ, Bonner PLR (2014) Modulation of transglutaminase 2 activity in H9c2 cells by PKC and PKA signaling: a role for transglutaminase 2 in cytoprotection. *Br J Pharmacol* 171: 3946-3960.

Arcaro A, Wymann MP (1993) Wortmannin is a potent phosphatidylinositol 3-kinase inhibitor: the role of phosphatidylinositol 3,4,5-trisphosphate in neutrophil responses. *Biochem. J.* 296: 297-301.

Benovic JL (2002) Novel  $\beta_2$ -adrenergic receptor signaling pathways *J Allergy Clin Immunol* 110: S229-S235.

Boros S, Ahrman E, Wunderink L, Kamps B, de Wong WW, Boelens WC, Emanuelsson CS (2006) Site-specific transamidation and deamidation of the small heat-shock protein Hsp20 by tissue transglutaminase. *Blood* 62: 1044-1052.

Caccamo D, Currò M, Lentile R (2010) Potential of transglutaminase 2 as a therapeutic target. *Expert Opin Ther Targets* 14: 989-1003.

Camps M, Rückle T, Ji H, Ardisson V, Rintelen F, Shaw J, Ferrandi C, Chabert C, Gillieron C, Francon B, Martin T, Gretener D, Perrin D, Leroy D, Vitte PA, Hirsch E, Wymann MP, Cirillo R, Schwarz MK, Rommel C (2005) Blockade of PI3K $\gamma$  suppresses joint inflammation and damage in mouse models of rheumatoid arthritis. *Nature Med* 11: 936-943.

Cordella-Miele E, Miele L, Beninati S, Mukherjee AB (1993) Transglutaminase-catalysed incorporation of polyamines into phospholipase A2. *J Biochem* 113: 164-173.

Csász E, Meskó B, Fésüs L (2009) Transdab wiki: the interactive transglutaminase substrate database on web 2.0 surface. *Amino Acids* 36: 615-617.

Daaka Y, Luttrell LM, Lefkowitz RJ (1997) Switching of the coupling of the  $\beta$ 2-adrenergic receptor to different G proteins by protein kinase A. *Nature* 390:88-91.

de Wit RJ, Hekstra D., Jastorff B, Stec WJ, Baraniak J, Van Driel R, Van Haastert PJ (1984) Inhibitory action of certain cyclophosphate derivatives of cAMP on cAMP-dependent protein kinases. *Eur J Biochem* 142: 255-260.

Donato R, Cannon BR, Sorci G, Riuzzi F, Hsu K, Weber DJ, Geczy CL (2013) Functions of S100 proteins. *Curr Mol Med* 13: 25-57.

Dudley, DT, Pang L, Decker SJ, Bridges AJ, Saltiel AR (1995) A synthetic inhibitor of the mitogen-activated protein kinase cascade. *Proc Natl Acad Sci USA* 92: 7686-7689.

Eckert RL, Kaartinen MT, Nurminskaya M, Belkin AM, Colak G, Johnson GVW, Mehta K (2014) Transglutaminase regulation of cell function. *Physiol Rev* 94: 383-417.

Freund KF, Doshi KP, Gaul SL, Claremon DA, Remy DC, Baldwin JJ, Pitzenberger SM, Stern AM (1994) Transglutaminase inhibition by 2-[(2-oxopropyl)thio]imidazolium derivatives: mechanism of factor XIIIa inactivation. *Biochemistry* 33: 10109-10119.

Gillet LC, Navarro P, Tate S, Röst H, Selevsek N, Reiter L, Bonner R, Aebersold R (2012) Targeted data extraction of the MS/MS spectra generated by Data-independent Acquisition: a new concept for consistent and accurate proteome analysis. *Mol Cell Proteomics* : 11(6), O111.016717.

Gundemir S, Colak G, Tucholski J, Johnson GVW (2012) Transglutaminase 2: a molecular Swiss army knife. *Biochim Biophys Acta* 1823: 406-419.

Hescheler J, Meyer R, Plant S, Krautwurst D, Rosenthal W, Schultz G (1991) Morphological, biochemical and electrophysiological characterization of a clonal cell (H9c2) line from rat heart. *Circ Res* 69: 1476-1486.

Huang Q, Yang L, Luo J, Guo L, Wang Z, Yang X, Jin W, Fang Y, Ye J, Shan B, Zhang Y (2015) SWATH enables precise label-free quantification on proteome scale. *Proteomics* 15: 1215-1223.

Hunter T (1995) When is a lipid kinase not a lipid kinase? When it is a protein kinase. *Cell* 83: 1-4.

Hwang KC, Gray CD, Sweet We, Moravec CS, Im MJ (1996)  $\alpha_1$ -adrenergic receptor coupling with G<sub>h</sub> in failing human heart. *Circulation* 94: 718-726.

Iismaa SE, Meams BM, Lorand L, Graham RM (2009) Transglutaminases and disease: lessons from genetically engineered mouse models and inherited disorders. *Physiol Rev* 89: 991-1023.

Iwai N, Shimoike H, Kinoshita M (1995) Genes up-regulated in hypertrophied ventricle. *Biochem. Biophys Res Commun* 209: 527-534.

Kase H, Iwahashi K, Nakanishi S, Matsuda Y, Yamada K, Takahashi M, Murakata C, Sato A, Kaneko M (1987) K-252 compounds, novel and potent inhibitors of protein kinase C and cyclic nucleotide-dependent protein kinases. *Biochem Biophys Res Commun* 142: 436-440.

Kimes BW, Brandt BL (1976) Properties of a clonal muscle cell line from rat heart. *Exp Cell Res* 98: 367-381.

Király R, Demény MA, and Fésüs L (2011) Protein transamidation by transglutaminase 2 in cells: a disputed  $Ca^{2+}$ -dependent action of a multifunctional protein *FEBS J.* **278**, 4717-4739.

Lambert J-P, Ivosev G, Couzens AL, Larsen B, Taipale M, Lin Z-Y, Zhong Q, Lindquist S, Vidal M, Aebersold R, Pawson T, Bonner R, Tate S, Gingras A-C (2013) Mapping differential interactomes by affinity purification coupled with data-independent mass spectrometry acquisition. *Nature Meth* 10: 1239-1245.

Lee KN, Arnold SA, Birkbichler PJ, Patterson Jr MK, Fraij BM, Takeuchi Y, Carter HA (1993) Site-directed mutagenesis of human tissue transglutaminase: Cys-277 is essential for transglutaminase activity but not for GTPase activity. *Biochim Biophys Acta* 1202:1-6.

Lilley GR, Skill J, Griffin M, Bonner PLR (1998) Detection of Ca<sup>2+</sup>-dependent transglutaminase activity in root and leaf tissue of monocotyledonous and dicotyledonous plants. *Plant Physiol* 117: 1115-1123.

Makitie LT, Kanerva K, Anderson LC (2009) Ornithine decarboxylase regulates the activity and localization of rhoA via polyamination. *Exp Cell Res* 315: 1008-1014.

Mishra S, Melino G, Murphy LJ (2007) Transglutaminase 2 kinase activity facilitates protein kinase A-induced phosphorylation of retinoblastoma protein. *J Biol Chem* 282: 18108-18115.

Mishra S, Murphy LJ (2006) Phosphorylation of transglutaminase 2 by PKA at Ser216 creates 14.3.3 binding sites. *Biochem Biophys Res Commun* 347: 1166-1170.

Naga Prasad SV, Jayatilleke A, Madamanchi, Rockman HA (2005) Protein kinase activity of phosphoinositide 3-kinase regulates  $\beta$ -adrenergic receptor endocytosis. *Nature Cell Biol* 7: 785-796.

Nanda N, Iismaa SE, Owens WA, Husain A, Mackay F, Graham RM (2001) Targeted inactivation of G<sub>i</sub>/tissue transglutaminase II. *J Biol Chem* 276: 20673-20678.

Nurminskaya MV, Belkin AM (2012) Cellular functions of tissue transglutaminase. *Int Rev Cell Mol Biol* 294: 1-97.

Okamoto T, Murayama Y, Hayashi Y, Inagaki M, Ogata E, Nishimoto I (1991) Identification of a G<sub>s</sub> activator region of the  $\beta$ 2-adrenergic receptor that is autoregulated via protein kinase A-dependent phosphorylation. *Cell* 67:723-730.

Perry MJ, Mahoney SA, Haynes LW (1995) Transglutaminase C in cerebellar granule neurons: regulation and localization of substrate cross-linking. *Neuroscience* 65: 1063-1076.

Rajagopal S, Ahn S, Rominger DH, Gowen-MacDonald W, Lam CM, DeWire SM, Violin JD, Lefkowitz RJ (2011) Quantifying ligand bias at seven-transmembrane receptors. *Mol Pharmacol* 80: 367-377.

Rockman HA, Koch WJ, Lefkowitz RJ (2002) Seven-transmembrane-spanning receptors and heart function. *Nature* 415:206-212.

Schaertl S, Prime M, Wityak J, Dominguez C, Munoz-Sanjuan I, Pacifici RE, Courtney S, Scheel A, Macdonald D (2010) A profiling platform for the characterization of transglutaminase 2 (TG2) inhibitors. *J Biomol Screen* 15: 478-487.

Schmitt JM, Stork PJS (2000)  $\beta_2$ -adrenergic receptor activates extracellular signal-regulated kinases (ERKs) via the small G-protein Rap1 and the serine/threonine kinase B-Raf. *J Biol Chem* 275: 25342-25350.

Shin DM, Kang J, Ha J, Kang HS, Park SC, Kim IG, Kim SJ (2008) Cystamine prevents ischaemia-reperfusion injury by inhibiting polyamination of RhoA. *Biochem Biophys Res Commun* 365: 509-514.

Singh RN, McQueen T, Mehta K (1995) Detection of the amine acceptor protein substrates of transglutaminase with 5-(biotinamido) pentylamine. *Anal Biochem* 231: 261-263.

Singh US, Kunar MT, Kao YL, Baker KM (2001) Role of transglutaminase II in retinoic acid-induced activation of RhoA-associated kinase-2. *EMBO J* 20: 2413-2423.

Slaughter TF, Achyuthan KE, Lai TS, Greenberg CS (1992) A microtiter plate transglutaminase assay utilizing 5-(biotinamido) pentylamine as substrate. *Anal Biochem* 205: 166-171.

Small K, Feng JF, Lorenz J, Donnelly ET, Yu A, Im MJ, Dorn GW 2<sup>nd</sup>, Liggett SB (1999) Cardiac specific overexpression of transglutaminase II (G<sub>h</sub>) results in a unique hypertrophy phenotype independent of phospholipase C activation. *J Biol Chem* 274: 21291-21296.

Smith PK, Krohn RI, Hermanson GT, Mallia AK, Gartner FH, Provenzano MD, Fujimoto EK, Goeke NM, Olson BJ, Klenk DC (1985) Measurement of protein using bicinchoninic acid. *Anal Biochem* 150:76-85.

Steinberg SF (1999) The molecular basis for distinct  $\beta$ -adrenergic receptor subtype actions in cardiomyocytes. *Circ Res* 85:1101-1111.

Szondy Z, Mastroberardino PG, Váradi J, Farrace MG, Nagy N, Bak I, Viti I, Wieckowski MR, Melino G, Rizzuto R, Tósaki A, Fesus L, Piacentini M (2006) Tissue transglutaminase (TG2) protects cardiomyocytes against ischemia/reperfusion injury by regulating ATP synthesis. *Cell Death Differ* 13: 1827-1829.

Trigwell SM, Lynch PT, Griffin M, Hargreaves AJ, Bonner PL (2004) An improved colorimetric assay for the measurement of transglutaminase (type II)-( $\gamma$ -glutamyl) lysine cross-linking activity. *Anal Biochem* 330: 164-166.

Vyas FS, Hargreaves AJ, Bonner PLR, Boocock D, Dickenson JM (2016) A<sub>1</sub> adenosine receptor-induced phosphorylation and modulation of transglutaminase activity in H9c2 cells: a role in cell survival. *Biochem Pharmacol* 107: 41-58.

Vlahos CJ, Matter WF, Hui KY, Brown RF (1994) A specific inhibitor of phosphatidylinositol 3-kinase, 2-(4-morpholinyl)-8-phenyl-4H-1-benzopyran-4-one (LY294002). *J Biol Chem* 269: 5241-5248.

Wang Y, Ande SR, Mishra S (2012) Phosphorylation of transglutaminase 2 (TG2) at serine-216 has a role in TG2 mediated activation of nuclear factor-kappa B and in downregulation of PTEN. *BMC Cancer* 12:277.

Yanagawa Y, Hiraide S, Matsumoto M, Shimamura K, Togashi H (2014) Enhanced transglutaminase 2 expression in response to stress-related catecholamines in macrophages. *Immunobiology* 219: 680-686.

Yano N, Ianus V, Zhao TC, Tseng A, Padbury JF, Tseng YT (2007) A novel signaling pathway for beta-adrenergic receptor-mediated activation of phosphoinositide 3-kinase in H9c2 cardiomyocytes. *Am J Physiol Heart Circ Physiol* 293: H385-H393.

Yu C-H, Chou C-C, Lee Y-J, Khoo K-H, Chang G-D (2015) Uncovering protein polyamination by the spermine-specific antiserum and mass spectrometric analysis. *Amino Acids* 47: 469-481.

Zamah AM, Delahunty M, Luttrell LM, Lefkowitz RJ (2002) Protein kinase A-mediated phosphorylation of the  $\beta$ 2-adrenergic receptor regulates its coupling to Gs and Gi: demonstration in a reconstituted system. *J Biol Chem* 277: 31249-31256.

Zhang W, Yano N, Deng M, Mao Q, Shaw SK, Tseng Y-T (2011)  $\beta$ -adrenergic receptor-PI3K signaling crosstalk in mouse heart: elucidation of immediate downstream signaling cascades. PLoS ONE 6(10): e26581. doi:10.1371/journal.pone.0026581.

Zhang Z, Vezza R, Plappert T, McNamara P, Lawson JA, Austin S, Pratico D, Sutton MSJ, FitzGerald GA (2003) COX-2 dependent cardiac failure in Gh/tTG transgenic mice. Circ Res 92: 1153-1161.

**Figure 1.**

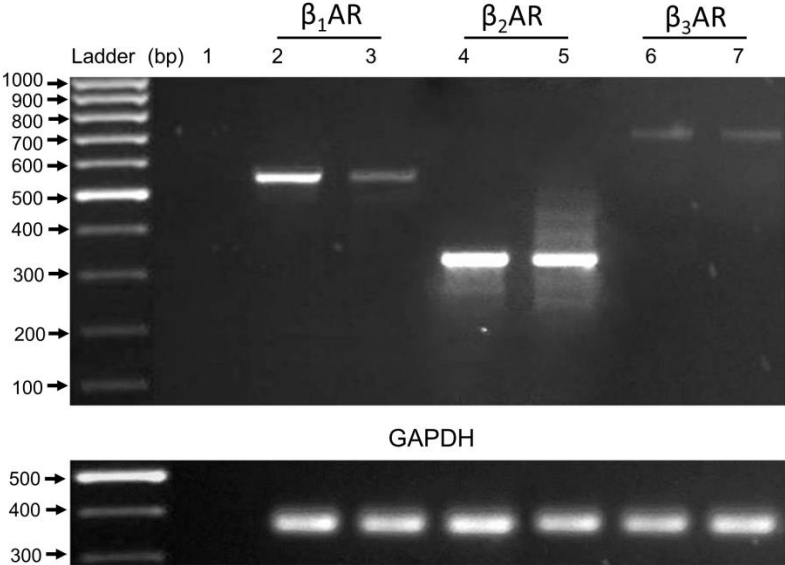


**Figure 2.**

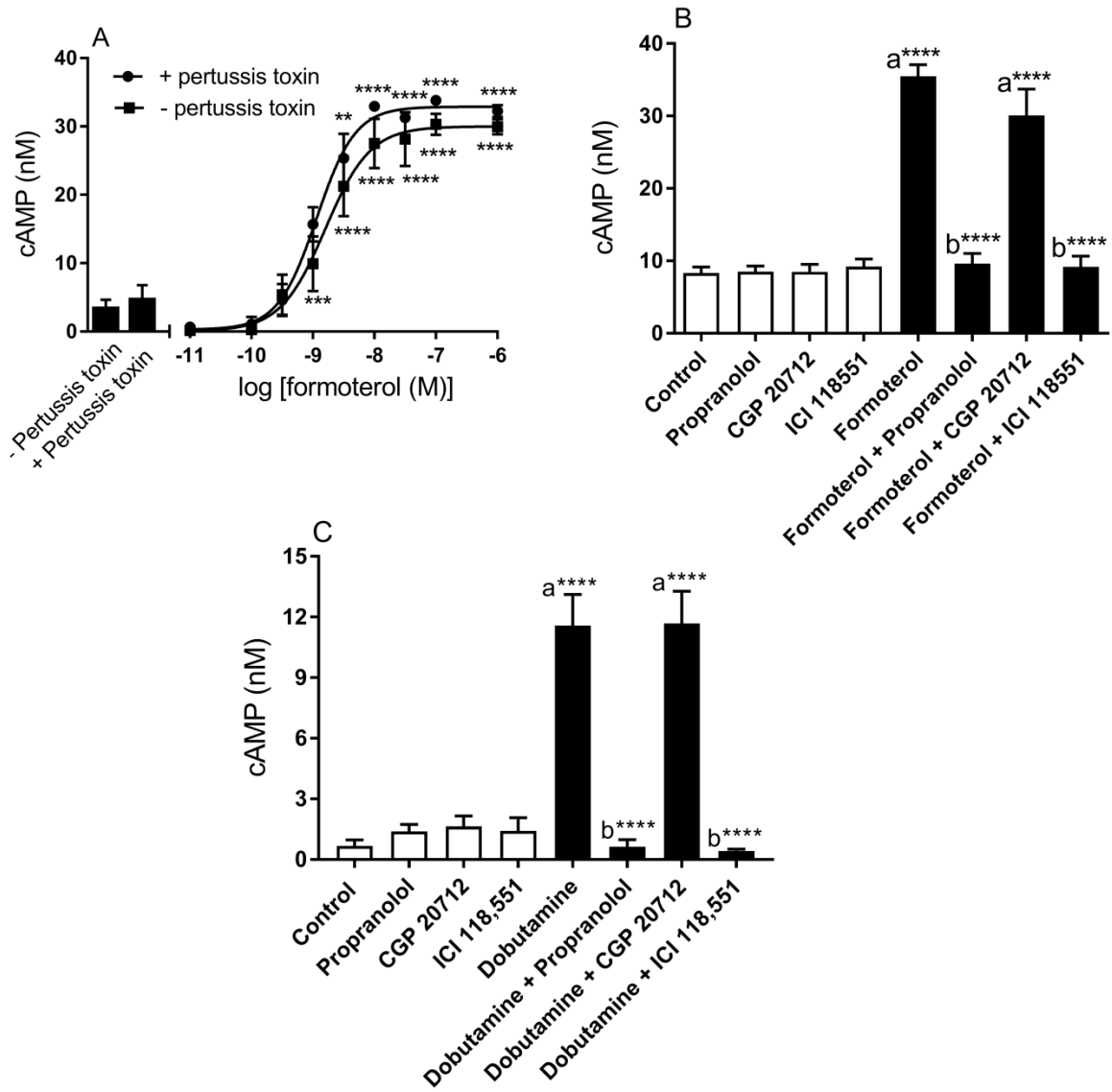


**Figure 3.**

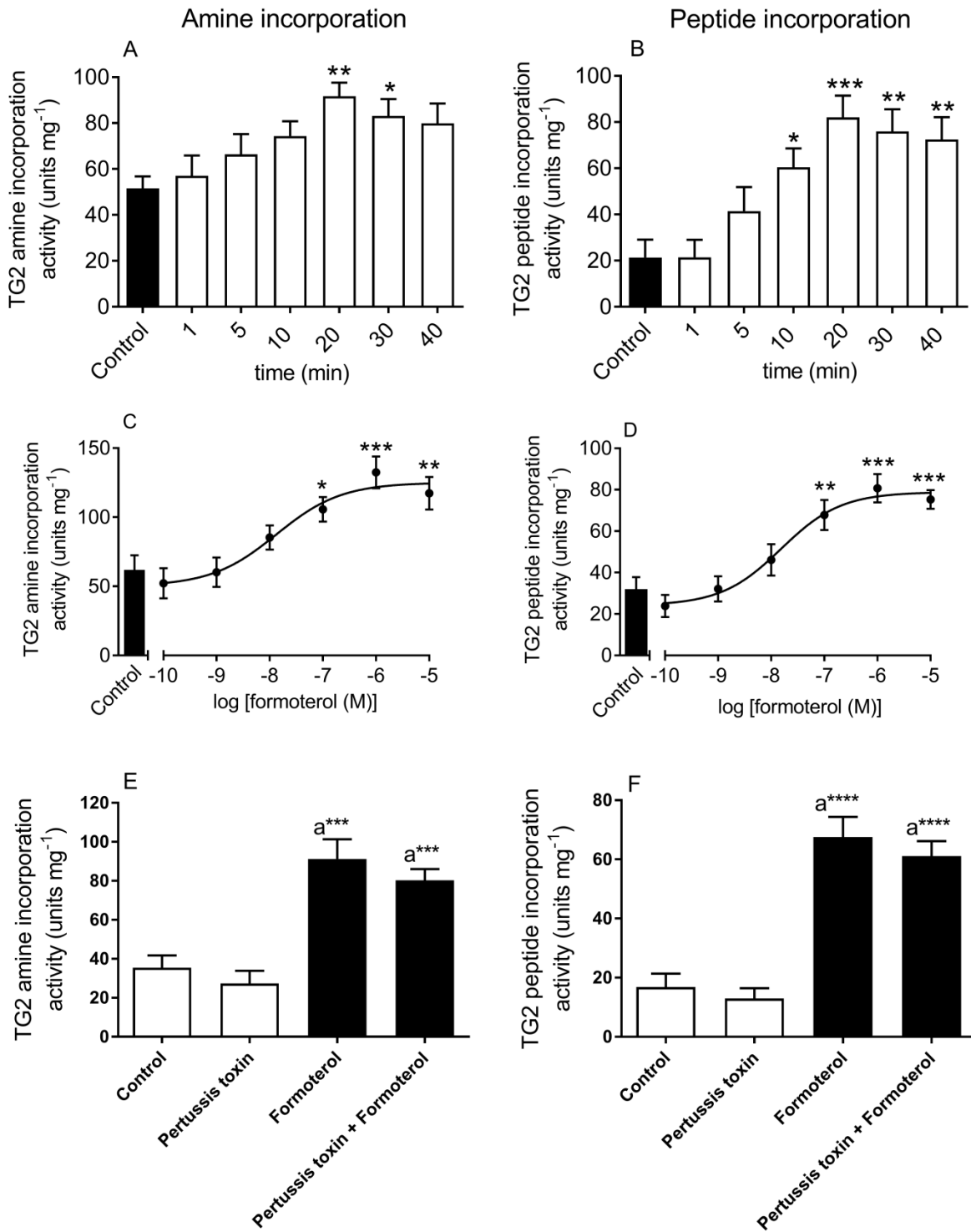


**Figure 4.**

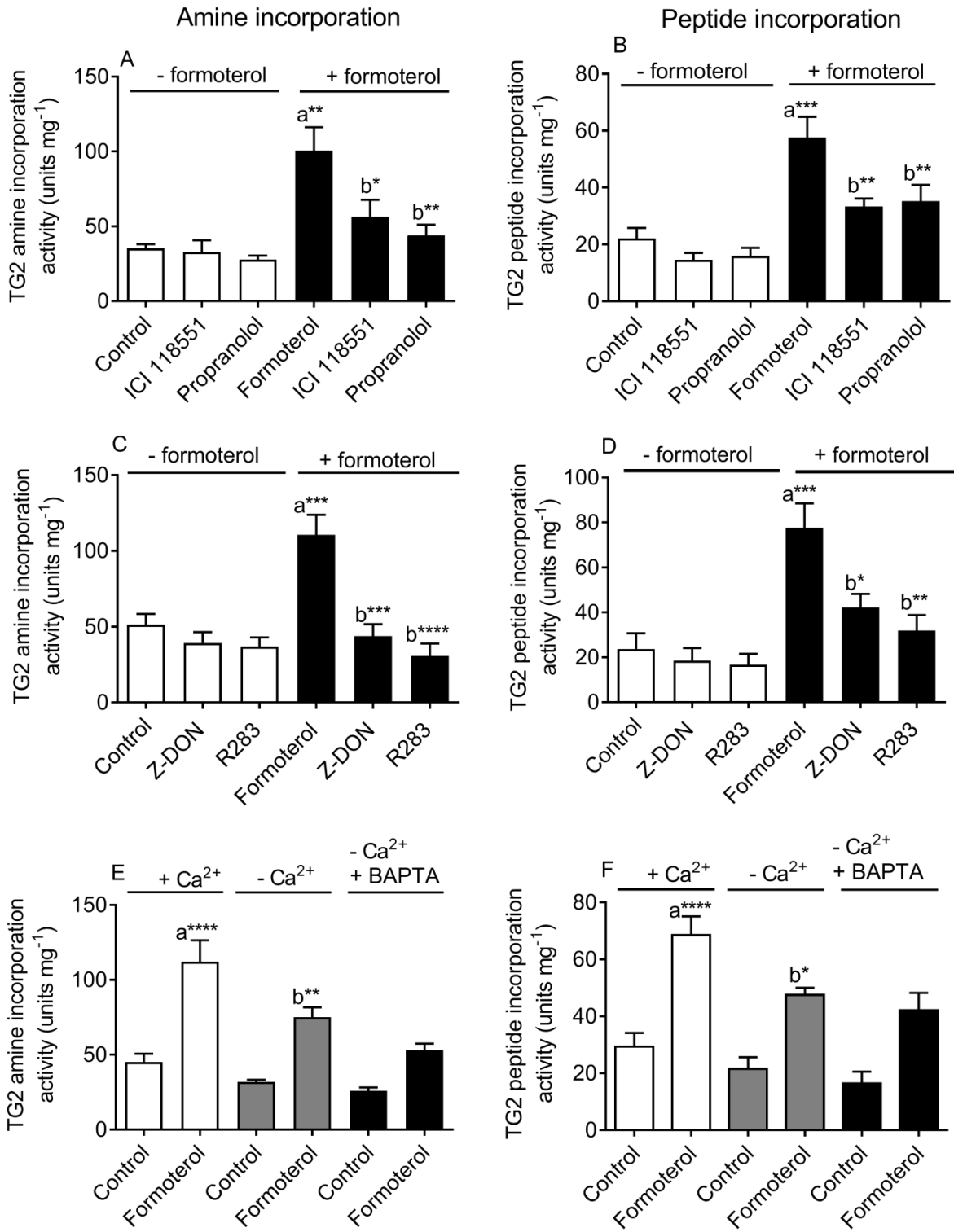


**Figure 5.**

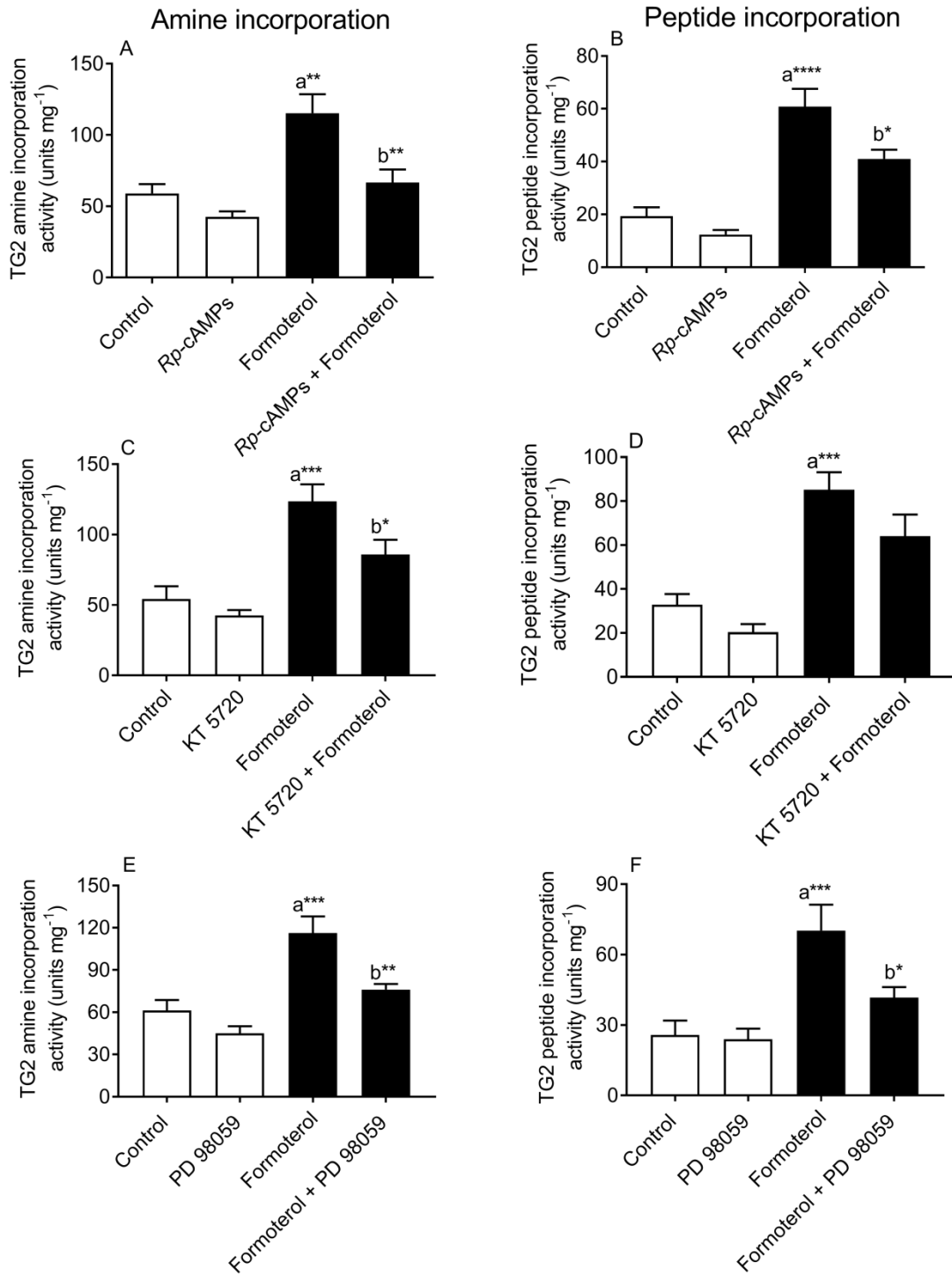


**Figure 6.**

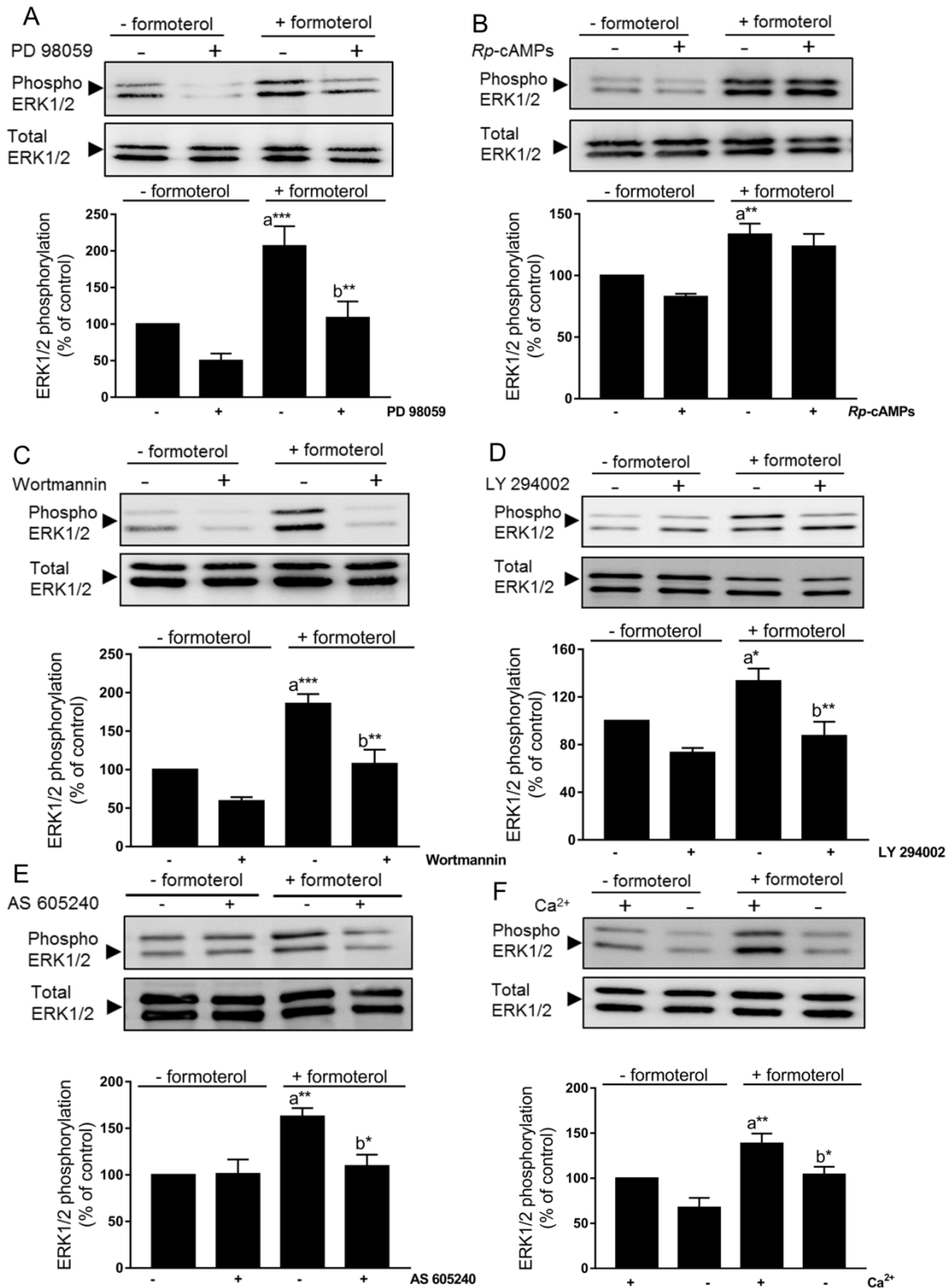


**Figure 7.**

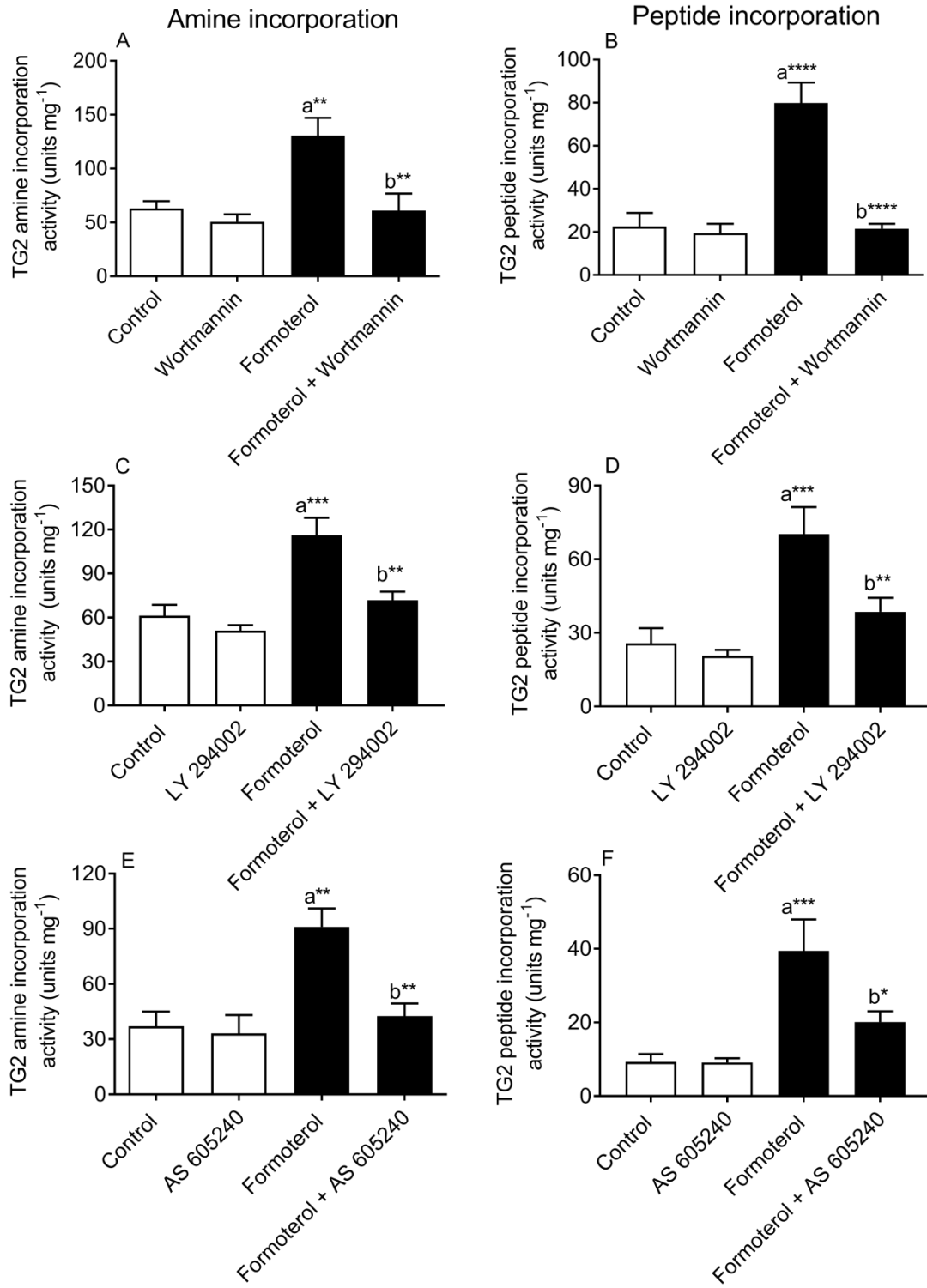


**Figure 8.**

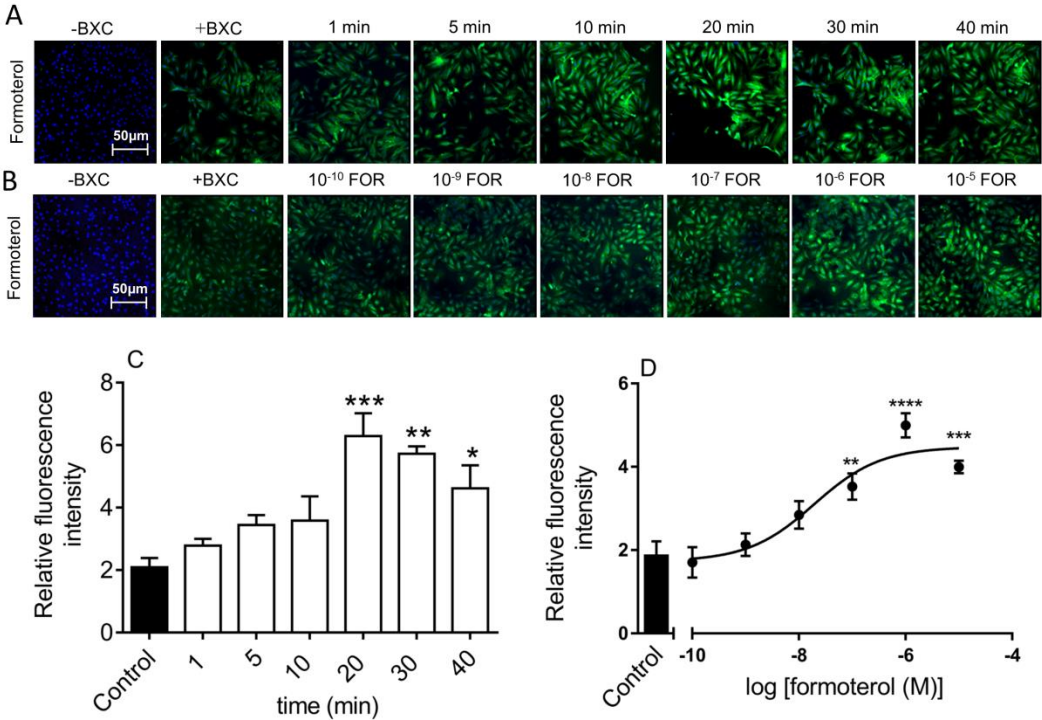


**Figure 9.**

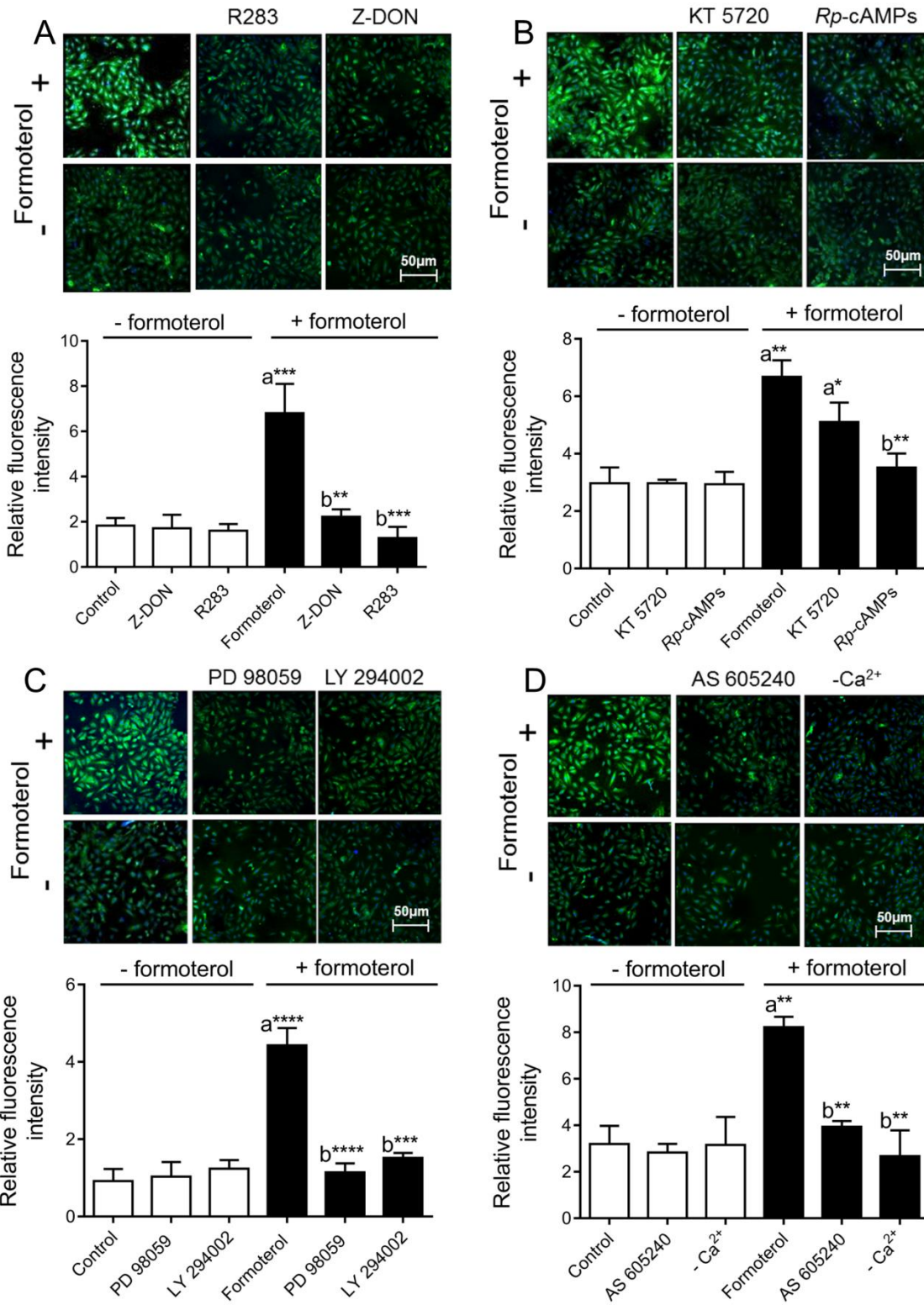


**Figure 10.**

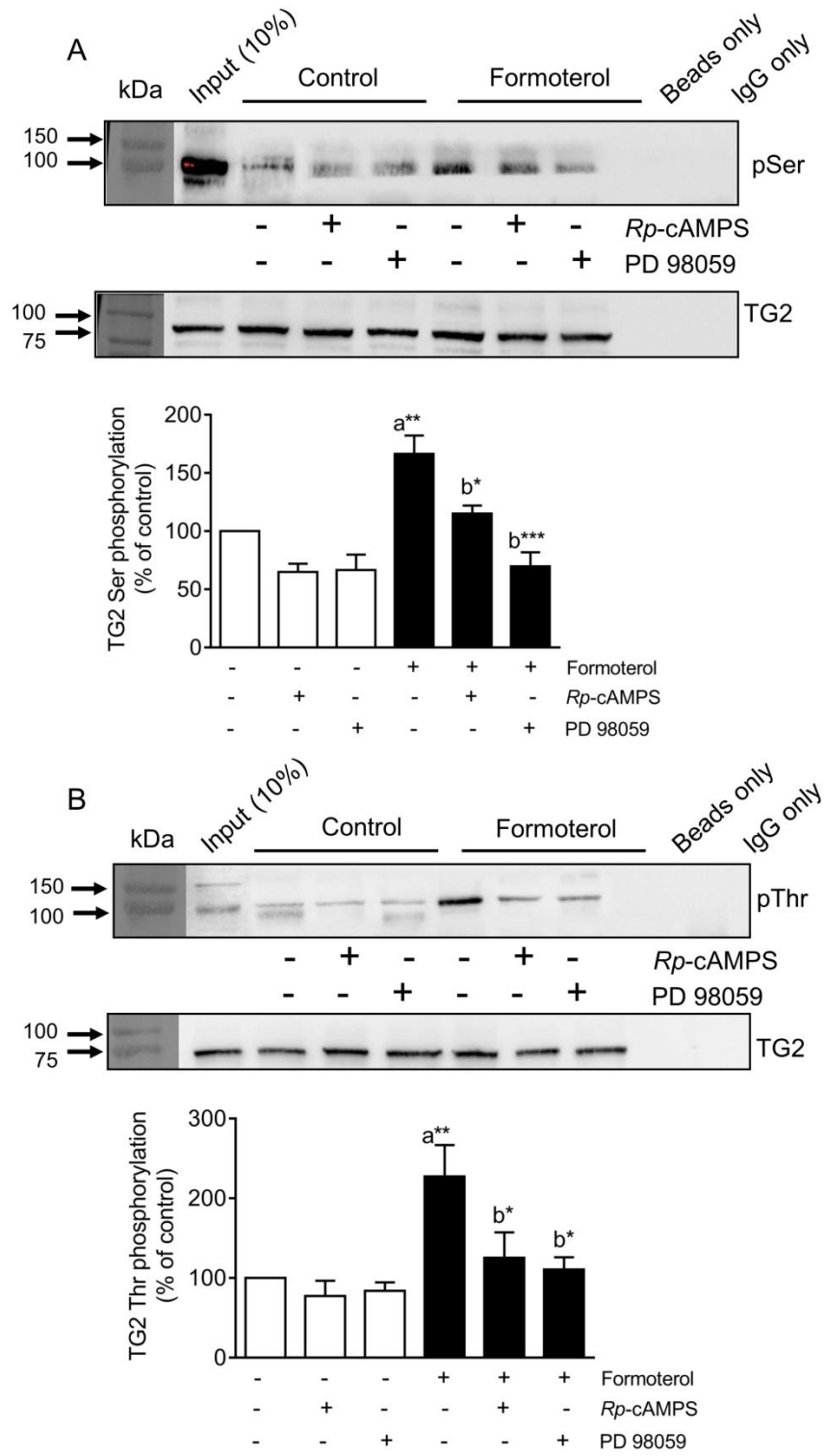


**Figure 11.**

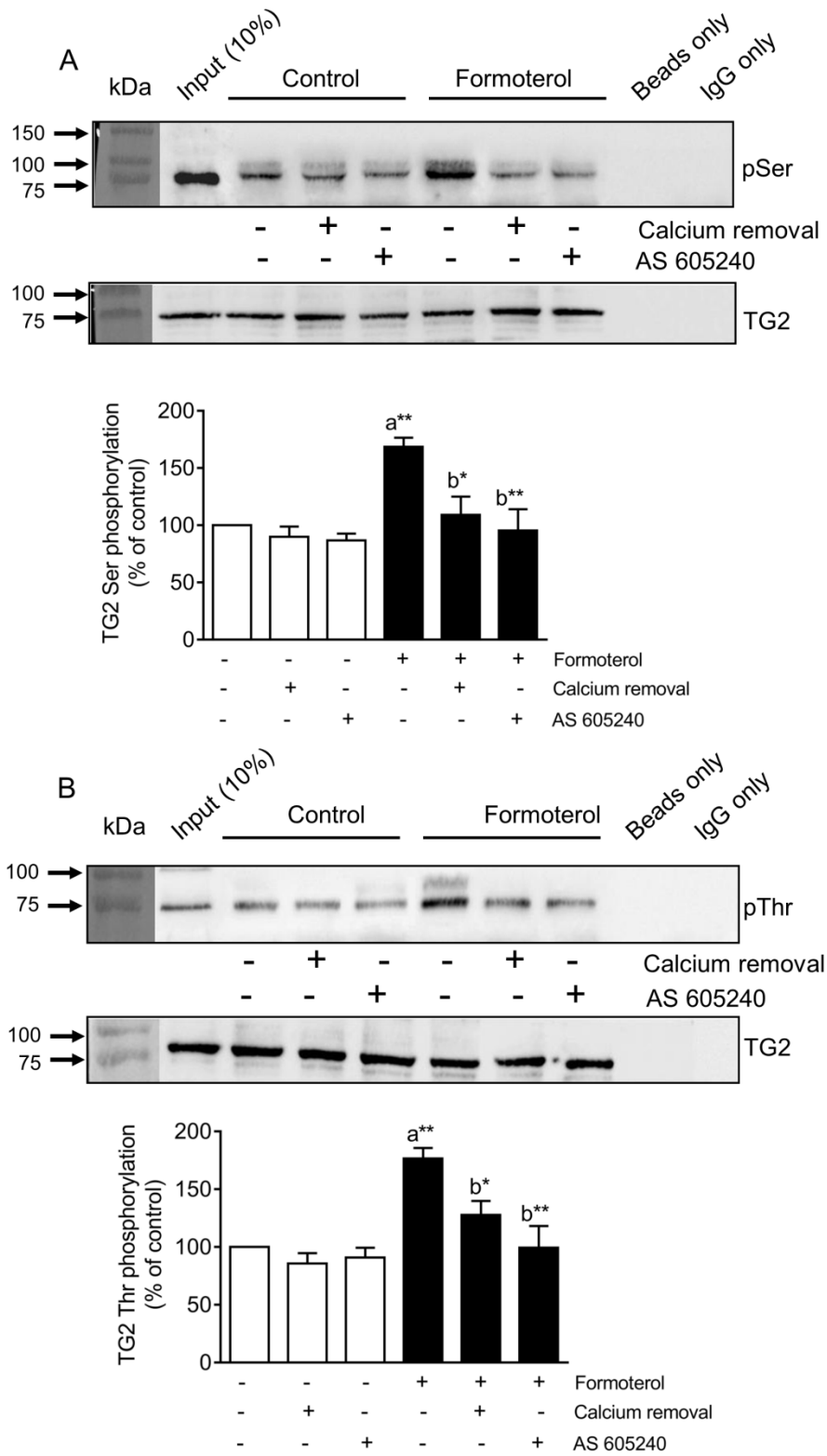


Figure 12.

